A simple, sensitive and quantitative FACS-based test for SARS-CoV-2 serology in humans and animals

Agnès Maurel Ribes[1+], Pierre Bessière[2+], Jean Charles Guéry[3], Eloïse Joly Featherstone[4], Timothée Bruel[5], Remy Robinot[5], Olivier Schwartz[5], Romain Volmer[2], Florence Abravanel[3,6], Jacques Izopet[3,6] and Etienne Joly[7 *]

1 : Laboratoire d'Hématologie, Centre Hospitalier Universitaire de Toulouse, 31000, Toulouse, France
2 : Ecole nationale vétérinaire de Toulouse, Université de Toulouse, ENVT, INRAE, IHAP, UMR 1225, Toulouse, France
3 : Institut Toulousain des Maladies Infectieuses et Inflammatoires (Infinity), Université de Toulouse, INSERM, CNRS, UPS, 31300 Toulouse, France
4 : York University Hospital, York YO31 8HE, UK
5: Institut Pasteur, Virus and Immunity Unit, CNRS-UMR3569, Paris, France
6: Université de Toulouse, INSERM, CNRS, UPS, 31300 Toulouse, France
7: Institute of Pharmacology and Structural Biology (IPBS), University of Toulouse, CNRS, Toulouse, 31000, France

+: AMR and PB made equivalent contributions to this work.
*: correspondence to EJ: atnjoly@mac.com

Abstract

Serological tests are important for understanding the physiopathology and following the evolution of the Covid-19 pandemic. Assays based on flow cytometry (FACS) of tissue culture cells expressing the spike (S) protein of SARS-CoV-2 have repeatedly proven to perform slightly better than the plate-based assays ELISA and CLIA (chemiluminescent immuno-assay), and markedly better than lateral flow immuno-assays (LFIA).

Here, we describe an optimized and very simple FACS assay based on staining a mix of two Jurkat cell lines, expressing either high levels of the S protein (Jurkat-S) or a fluorescent protein (Jurkat-R expressing m-Cherry, or Jurkat-G, expressing GFP, which serve as an internal negative control). We show that the Jurkat-S&R-flow test has a much broader dynamic range than a commercial ELISA test and performs at least as well in terms of sensitivity and specificity. Also, it is more sensitive and quantitative than the hemagglutination-based test HAT, which we described recently. The Jurkat-flow test requires only a few microliters of blood; thus, it can be used to quantify various Ig isotypes in capillary blood collected from a finger prick. It can be used also to evaluate serological responses in mice, hamsters, cats and dogs. Whilst the Jurkat-flow test is ill-suited and not intended for clinical use, it offers a very attractive solution for laboratories with access to tissue culture and flow cytometry who want to monitor serological responses in humans or in animals, and how these relate to susceptibility to infection, or re-infection, by the virus, and to protection against Covid-19.

Note: This manuscript has been refereed by Review Commons, and modified thanks to the comments and suggestions from two referees. Those comments, and our replies, are provided at the end of the manuscript's pdf, and can also be accessed by clicking on the box with a little green number found just above the "Abstract " tab in the medRXiv window.

Introduction

Over the past year, our world has been thrown into disarray by a pandemic caused by a new coronavirus, SARS-CoV-2. With a mortality rate around 1%, this new virus is not as pathogenic as previous coronaviruses such as SARS-CoV (9.6%) and MERS (35%), but it transmits faster from human-to-human (Fani et al., 2020), probably because of a large proportion (ca. 50%) of asymptomatic carriers (Long et al., 2020; Wu et al., 2021). Consequently, in less than two years since its discovery in Wuhan, China, SARS-CoV-2 has spread all over the world and caused more than 200 millions confirmed cases and over 4 millions confirmed deaths (https://www.who.int/emergencies/diseases/novel-coronavirus-2019).

Biotechnology has proven a great asset in combating the pandemic, with the rapid development of diagnostic tests and, more recently, of vaccines. Diagnostic tests detect directly either the viral nucleic acid or viral proteins in nasopharyngeal swabs. Serological tests, by contrast, detect antibodies developed in response to infection by the virus or vaccination, or a combination of the two. Since the presence of antibodies in serum usually correlates with elimination of the virus and the patient's recovery, serological tests have not been very helpful in the clinic. They have, however, proven an essential tool to follow the spread of the pandemic by evaluating seroprevalence in populations, and they are now set to become essential to evaluate the immunity of individuals as well as populations (Koopmans and Haagmans, 2020).

Whilst several thousands of serological studies have been published by now, based on tests performed in many millions of individuals, those myriad studies mostly document the seroprevalence in certain populations at a given time (Chen et al., 2021), but information

regarding the actual protection afforded by immunity after infection by SARS-CoV-2, and how this correlates with the presence of antibodies against the SARS-2 virus is only just starting to come out (Abu-Raddad et al., 2021; Garcia-Beltran et al., 2021; Harvey et al., 2021a; Jeffery-Smith et al., 2021; Letizia et al., 2021; Lumley et al., 2021).).

While these recent publications show that the presence of antibodies does correlate with protection against the Covid-19 disease, and in particular against the more serious forms of the disease, one of the more burning questions that remains to be answered is how long this protection will last? Another crucial question concerns whether there will be differences in the duration of this protection depending on which vaccine was used, and whether an individual had been infected by the SARS-CoV-2 virus before, or after, being vaccinated.

Obtaining answers to this type of questions should be greatly facilitated by access to simple, cheap and quantitative serological tests, which would work both in humans and in animal models. To date, however, although a multitude of commercial serological tests have been developed to detect the presence of antibodies in the serum of patients (Farnsworth and Anderson, 2020), those are mostly ill-suited for use in research laboratories, not only because of their price, but also because they are not or only poorly quantitative.

The most commonly used methods for Covid-19 serodiagnostic are either ELISA (Enzyme-Linked ImmunoSorbent Assays) or CLIA (ChemiLuminescent ImmunoAssays). Whilst those methods show very good sensitivity and specificity, they also have several significant drawbacks:

i) The commercial versions are based on using volumes of serum or plasma which exceed the amounts which can be readily obtained by finger prick, and therefore require venipuncture, and hence trained personnel to collect the samples, and elaborate logistics to handle those samples.
ii) They are relatively expensive (ca. 500 € per plate of 90 tests for commercial ELISA or CLIA) and not easily modular (i.e. a whole plate will often have to be used even if only a few tests are to be performed). Whilst in-house ELISAs are a possible alternative, they are difficult to standardize and require high amounts of recombinant antigen (Amanat et al., 2020).
iii) Whilst ELISA tests are quantitative, they tend to saturate rapidly, and thus show a relatively limited dynamic range.
iv) Most commercial versions are designed to detect human antibodies, and thus cannot be used to follow serological responses in animal models.

Early in the pandemic, because they could be used in a point of care setting on capillary blood obtained by finger pricks, lateral-flow immune assays (LFIA) attracted considerable attention as an alternative to the ELISA or CLIA plate-based methods. Dozens of versions were developed by various commercial companies, and despite their relatively high price, such LFIAs were used in scores of studies to evaluate the prevalence of sero-conversion in various populations. Over time, however, the general performances of LFIAs have proven to be too low, both for sensitivity and reliability, to be of real use in clinical settings, and even for epidemiological studies (Adams et al., 2020; Dortet et al., 2021; Mohit et al., 2021; Moshe et al., 2021).

As an alternative to those various serological tests, we set out to develop a serological test based on hemagglutination, with the aim of obtaining a method that would be both sensitive, cheap, and could be used both in the laboratory, in field settings or as a point of care test,

115 without the requirement for any elaborate equipment. The HAT (HemAgglutination Test) method
116 is based on a single reagent, IH4-RBD, which binds to human red blood cells (RBC) via the IH4
117 nanobody specific for human Glycophorin A and coats them with the RBD domain of the SARS-
118 CoV-2 virus (Townsend et al. 2021). HAT has a sensitivity of 90% and specificity of 99%, and is
119 now used by several laboratories worldwide for epidemiological and clinical studies
120 (Ertesvåg et al., 2021; Jayathilaka et al., 2021; Jeewandara et al., 2021; Kamaladasa et al., 2021).
121 To be able to perform HAT on whole blood with the sensitivity and simplicity which we set out
122 the reach, and to attempt to make it quantitative, various modifications and improvements had
123 to be tested, and in order to do this, we felt that we needed a simple quantitative test that
124 would allow us to evaluate the amount of antibodies present in the whole-blood samples we
125 were using more simply and cheaply than by using ELISA or CLIA. Thanks to the use of the Jurkat-
126 S&R-flow test, we have now managed to derive an adapted protocol of the HAT test called HAT-
127 field, which can provide a serological quantitative evaluation of the antibodies directed against
128 the SARS-CoV-2 RBD is a single step, starting from a few microliters of blood such as can be
129 obtained by a finger-prick, and requires absolutely no specialized equipment
130 (Joly and Maurel Ribes, 2022)
131
132 For validating the adaptation of the HAT test, we had initially turned to the S-flow test
133 (Grzelak et al., 2020), which uses flow cytometry (FACS) performed on human cells expressing
134 the S protein. The S-flow test appeared as a very promising approach since it is very simple to run
135 and its performances compared favorably with three other serological tests (two ELISA directed
136 towards the S or N proteins, and a luciferase immuno- precipitation system (LIPS) combining
137 both N and S detection).
138 The S-flow method initially described used HEK cells (Grzelak et al., 2020), which are adherent
139 cells. We felt that it would be better to use cells growing in suspension, not only because it
140 makes it a lot easier to grow large numbers of cells, but also because those can be used directly,
141 without having to be detached from the plastic, which we feared could possibly alter the cells'
142 characteristics, and introduce a possible source of variability between assays.
143 In this regard, Horndler and colleagues have recently described an assay inspired by the S-flow
144 assay, but based on Jurkat cells expressing both the full-length native trimeric S-protein of SARS-
145 CoV-2 and a truncated form of the human EGFR protein, which is used as an internal control for
146 the expression level of the S protein (Horndler et al., 2021).
147 One of the caveats of using human cells to express the S protein, however, is that those cells
148 will also express other antigens, and MHC molecules in particular, which can be the targets of
149 allo-reactive antibodies present in certain individuals, and not others. The background level of
150 staining on Jurkat cells themselves will thus vary from sample to sample. To circumvent this
151 difficulty, Pinero et al. have used the Jurkat-S+EGFR cells mixed with untransfected Jurkat cells as
152 negative controls (Piñero et al., 2021).
153 Having followed the same reasoning as Horndler *et al.*, we had chosen to make use of Jurkat
154 cells expressing the native trimeric form of the spike protein of the SARS-CoV-2 virus, but we
155 elected to use Jurkat cells expressing the mCherry red fluorescent protein as negative controls.
156 This is not only cheaper because it does not require labelling the cells with an additional
157 commercial antibody, but also has the advantage of using two cell lines that are maintained in
158 the same selective tissue culture medium.
159 In all three papers (Grzelak et al., 2020; Horndler et al., 2021; Piñero et al., 2021), and several
160 others

(Egia-Mendikute et al., 2021; Goh et al., 2021; Hambach et al., 2021; Lapuente et al., 2021), the sensitivity of approaches based on flow cytometry was reported to be superior to those of ELISA or CLIA, probably because such tests are based on detecting the spike protein expressed in its native conformation.

Since the Jurkat-flow test calls for the use of both a flow cytometer and cells obtained by tissue culture, it is clearly not destined to be used broadly in a diagnostic context, but its simplicity, modularity, and performances both in terms of sensitivity and quantification capacities should prove very useful for research labs working on characterizing antibody responses directed against SARS-2, both in humans and animal models.

Results and Discussion

Jurkat-S&R-flow: basic principles

Jurkat cells expressing high levels of the SARS-CoV-2 spike protein, which we subsequently refer to as Jurkat-S, or J-S, were obtained by means of transduction with a lentiviral vector, followed by three rounds of cell sorting. A second population of Jurkat cells, in which all cells express the mCherry fluorescent protein, and which we subsequently refer to as Jurkat-R, or J-R, was also obtained by lentiviral transduction (see M&M: Materials and Methods section).

For the Jurkat-S&R-flow test, we simply prepare a mix of equivalent numbers of the two cells lines, J-S and J-R, and use either sera or plasma at a final dilution of 1/100 to label 2.10^5 cells of this mix (see M&M for details). After this primary step of labelling, the cells are washed before being incubated with a fluorescent secondary antibody, and a final wash is performed before analysis by flow cytometry.

The advantage of using such an approach is that it guarantees that the test cells (Jurkat-S) and the control cells (Jurkat-R) are labelled in exactly the same conditions. Comparing the levels of staining between test and control cells can then be carried out without any risk of a difference between the two being due to a difference in the course of the labelling procedure (e.g. certain samples receiving less of the primary or secondary antibodies). Accessorily, another significant advantage of such an approach is that it reduces the number of FACS samples to be processed by a factor of two.

The mCherry signal allows simple separation by gating during analysis of the control cells from the test cells (Figure 1). In samples labelled just with the secondary antibody (neg. cont.) or with pre-pandemic plasma which does not contain antibodies against the spike protein (neg plasma), similar green signals are found on J-S et J-R populations. When there are antibodies against the spike protein present in the plasma or serum used to label the cells, this will result in a marked difference in the green signals detected on the J-S cells compared to the J-R cells. The difference in the fluorescence intensity between the two populations will provide a quantitative evaluation of the amounts of antibodies in the serum or plasma used to label the cells (first column). The numbers shown in red correspond to the relative specific staining (RSS = signal J-S – signal J-R / signal neg. cont.).

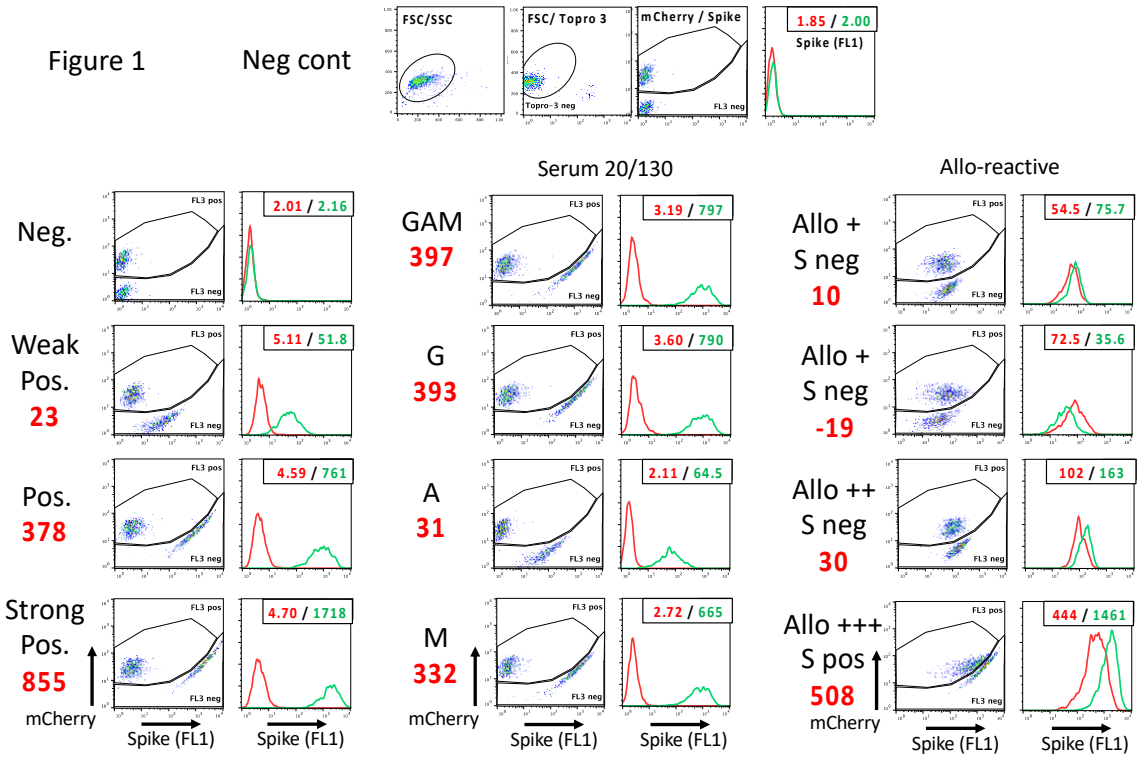

Figure 1: <u>Basic principle and examples of the Jurkat-S&R-flow test</u>

A 50/50 mix of Jurkat cells expressing either the S protein of the SARS-CoV-2 virus or the mCherry protein is first incubated with a 1/100 dilution of the plasma or serum sample to be tested, followed by incubation with a green fluorescent secondary antibody. The cells are then analyzed by flow cytometry.

The panels on the first line show the gating strategy, using as an example the sample of a negative control, stained only with an anti-human pan specific secondary antibody conjugated to alexa-488 : Live cells are first selected on a combination of two gates drawn on three parameters: size (FSC), granularity (SSC), and far red fluorescence (FL4) to eliminate the dead cells labelled by the Topro3 live stain. Jurkat-S are then distinguished from Jurkat-R cells using the red fluorescence of the latter, by means of a gate drawn on a FL1/FL3 dotplot. The gates had to be drawn that way to accommodate the fact that, for the brightest cells, the green fluorescent signal of alexa-488 can 'bleed' into the FL3 channel, and the Cellquest software does not allow for FL3/FL1 compensation. A histogram overlay is then drawn with the cells falling in each of these two gates (red: Jurkat-R, green: Jurkat-S). The numbers in the upper right corners of those histograms correspond to the GMFIs of the two histograms.

The red numbers shown to the left of the plots correspond to the relative specific staining (RSS; i.e. the difference of signal between J-S and J-R divided by the GMFI of the negative control, i.e. 2.00)

The first column shows examples of staining with 4 different plasmas which were either negative, or weakly, positively and strongly reactive with the spike protein.

The second column shows an example of the Jurkat-S&R-flow test capacity to perform a rough evaluation of the relative proportion of the various Ig isotypes in a sample, in this case the 20/130 reference serum obtained from the NIBSC, which contains 476 IgG BAU (binding antibody units) according to the data sheet provided with the antibody.

The third column presents examples of some of the rare samples which showed various levels of allo-reactivity against the Jurkat cells themselves. Although the sample on the third line had an RSS of 30 (thus well above the threshold of 20 set for positivity), this sample was probably negative since it showed no reactivity in the other two serological tests. The sample on the fourth line shows that some sera can be both allo-reactive against the Jurkat cells, and strongly reactive against the spike protein.

233 If isotype-specific secondary reagents are used, an evaluation of the respective amounts of
234 various classes of antibodies can also be obtained (second column). It should, however, be noted
235 that, because different secondary reagents do not necessarily recognize the various Ig isoforms
236 with the same efficiency, this provides only a very rough analysis of the relative amounts of Ig-G,
237 -A and -M. Within a set of samples, however, this can provide very simple means to compare
238 samples with one another (Table S1).
239
240 As alluded to in the introduction, one of the possible caveats of using a human cell line to
241 express the S protein is that some blood samples will contain allo-reactive antibodies directed
242 against that cell line, possibly as a consequence of a pregnancy, or past history of receiving a
243 blood transfusion or organ transplant (Hickey et al., 2016; Karahan et al., 2020). The third column
244 of Figure 1 shows examples of such samples containing marked levels of alloreactive antibodies,
245 i.e. samples for which the J-R cells show significant levels of staining compared to the same cells
246 labelled with just the secondary antibody. Based on our results collected on more than 350
247 clinical samples, we evaluate that ca. 30 % of samples will contain allo-reactive Abs that will
248 result in levels of staining of Jurkat cells that are more than five-fold that of the signal obtained
249 for the negative control (and 3-6 % more than ten-fold). Of note, we did not notice an increased
250 frequency of allo-reactivity in samples from women compared to men, which suggests that allo-
251 reactivity after pregnancy is not a major cause in the origin of those allo-reactions.
252
253 A difficult question with all serological tests is that of where to set the threshold beyond
254 which the specific signals detected can confidently be considered as positive, which will be
255 directly linked to the balance between sensitivity and specificity of the assay. Based on the
256 analyses of various cohorts of positive and negative samples (some of which will be presented
257 further down in this manuscript), for the Jurkat-S&R-flow, we have settled for a threshold of RSS
258 =20, i.e. twenty-fold the value of the negative control stained just with secondary-antibodies.
259 The reason for using the geometric mean of fluorescence intensity (GMFI) of the negative control
260 as an internal reference is that, in flow cytometry, the numerical values of fluorescence
261 intensities will be totally dependent upon the cytometer settings, and the voltages applied to the
262 PMT in particular. But we find that this can be somewhat compensated by such an approach. For
263 example, in the conditions used in our experiments, the GMFI of the negative control had a value
264 of ca. 2 when analyzed on a FACScalibur flow cytometer. With a threshold set at 20, samples
265 were thus considered as positive if the difference in the GMFI of the J-S and J-R populations was
266 above 40 (numbers shown in red in Figure 1 are J-S – J-R / 2). When the very same samples were
267 analyzed on a Fortessa flow cytometer (Figure S1), the value of the GMFI for the negative control
268 was 24-fold higher, but the RSS values obtained closely resembled those obtained with the same
269 samples on the FACScalibur (red numbers in Figure S1 and Figure 1: 20/23; 366/378; 916/855;
270 490/508).
271
272 For the samples showing high levels of allo-reactive staining, however, it is worth underlining
273 that this threshold of 20 had to be considered with some caution. Indeed, in those allo-reactive
274 samples, such as the examples shown in the right column of Figure 1, we found that the
275 difference between the green signals recorded for the J-S and J-R populations can fluctuate
276 between experiments, presumably because those signals correspond to the recognition by allo-
277 reactive antibodies of cell surface markers that are not always expressed at the same levels in all
278 Jurkat cells. Such alloreactive signals can be higher in J-R for certain serum or plasma samples, or

279 in J-S for other samples (first vs second and third line), without, in this latter case, necessarily
280 corresponding to bona-fide reactivity against the spike protein of the SARS-CoV2 virus. The
281 sample shown on the fourth line represents the most extreme case we have come across, from a
282 Covid-19 patient with extremely high allo-reactivity, coupled to bona fide reactivity against the
283 spike protein. All in all, it is simply worth underlining that, for the small percentage of samples
284 showing significant alloreactivity against Jurkat cells, and staining of Jurkat-S slightly higher than
285 that of Jurkat-R, their reactivity should be checked with a different serological test before
286 considering them as truly positive.
287
288 Inspection of the dot plot for this very alloreactive sample provides the explanation for the
289 slightly odd shapes of the FL1/FL3 gates we used to discriminate Jurkat-S from Jurkat-R cells. This
290 was necessary because, on the FACScalibur, the fluorescent signal of mCherry is best captured by
291 the FL3 channel, but the version of the Cellquest program used for acquisition on this cytometer
292 does not allow for FL3/FL1 compensation. Consequently, samples with extremely high FL1 signals
293 showed some 'bleeding' into the FL3 channel. We found that this could not be satisfactorily
294 treated by post-acquisition compensation with the Flowjo analysis software either, and thus
295 resorted to drawing such gates to separate J-S from J-R populations.
296
297 We had elected to use a green/red combination for test and control cells for two reasons: 1)
298 secondary antibodies labeled with green fluorescent dyes such as fluorescein or Alexa 488 are
299 the most commonly available, and also usually the cheapest. 2) All flow-cytometers, even the
300 most basic ones, are equipped with a 488 nm laser which allows to perform green/red analyses.
301 Another important consideration is that one of the goals of this study was to set up a test which
302 could be used by as many research teams as possible, including those based in institutes from
303 less affluent countries, which are less likely to have access to recent, state-of-the-art multi-laser
304 flow cytometers. As will be seen later, with secondary antibodies conjugated to Alexa-647 which
305 can be excited by the second 633 nm laser of the FACScalibur, it is possible to use Jurkat-GFP
306 cells as an alternative to J-R cells.
307
308 When the same samples as shown on Figure 1 were analyzed using a Fortessa flow cytometer,
309 the picture was quite different (Figure S1). This more recent flow cytometer is endowed with
310 several lasers, including a 561 nm Yellow-Green laser, which is much better suited for the
311 excitation of the mCherry fluorescent protein, thus yielding much higher signals which, since they
312 are acquired on a different laser line from the green signals, require absolutely no compensation.
313
314 In many flow cytometry facilities, users are required to fix any samples that have been in
315 contact with materials of human origin. Whilst this was not the case for us, we still tried
316 analyzing the same samples after those were fixed with 1% formaldehyde and kept for 4 days at
317 4°C before re-analysis. As can be seen on the right part of Figure S1, formaldehyde-fixation
318 resulted in a 7-fold drop in the intensity of the mCherry signals, which made it impossible to
319 separate J-R from J-S populations on the FACScalibur (first line). On the other hand, analysis on
320 the Fortessa was still comfortably possible. Of note, whilst formaldehyde did not noticeably alter
321 the fluorescence signals of the alexa-488 dye, it did result in a twofold increase of the green
322 auto-fluorescence of the negative controls, hence resulting in a twofold reduction of the RSS
323 compared to those obtained on unfixed cells.

324 ***Performance of the JurkatS&R-flow test on clinical samples***
325
326 Next, we compared the performance of the Jurkat-S&R-flow test with those of two other
327 serological tests: the Wantai commercial RBD ELISA test, and the hemagglutination-based test,
328 HAT (Townsend et al., 2021).
329
330 For this, we made use of two cohorts of clinical samples.
331 First, a preexisting cohort of 121 sera available in the virology laboratory of the Toulouse
332 hospital which had all previously been tested with the Wantai RBD ELISA test
333 (Abravanel et al., 2020), comprising 40 negative serum samples collected before December 2020,
334 and 81 sera from PCR-positive subjects. For those samples, RBCs from O- donors were used to
335 perform the HAT tests (see M&M).
336 The second cohort consisted of 267 whole blood samples collected on EDTA, obtained from
337 the hematology department of the Toulouse hospital as left-over clinical material, for which we
338 have consequently very little clinical information. For those samples, the HAT test was performed
339 on whole blood, i.e. using the subjects' own RBCs for hemagglutination. The blood samples were
340 subsequently centrifugated, and the plasmas collected to perform the Jurkat-S&R-flow and the
341 RBD-ELISA tests.
342
343 The result of the analysis of these two cohorts with the three serological tests are presented
344 in Figure 2, with colors used to represent the HAT results.
345

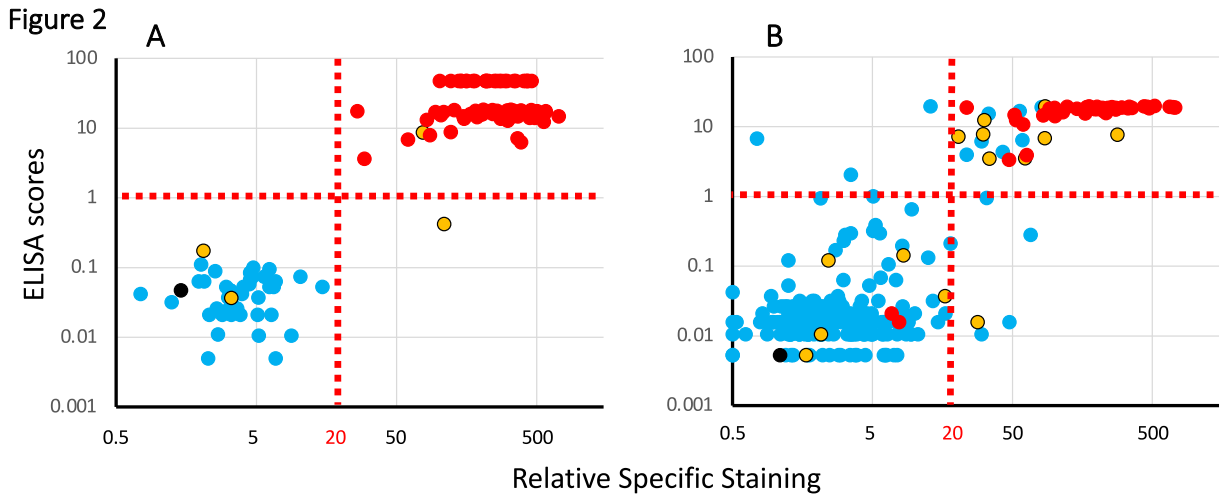

346
347
348 **Figure 2**: Comparison of the results of the 3 serological tests on two cohorts of clinical samples.
349 Panel A: results obtained with a cohort of 121 serum samples (81 PCR pos, 40 neg) collected by the
350 virology department of the Purpan Hospital (Toulouse, France).
351 Panel B: results obtained with a cohort of 267 whole blood samples coming from the hematology
352 department of the Rangueil Hospital (Toulouse, France).
353 Each plot presents ELISA scores (Y axis) against the results of the Jurkat-S&R-flow tests, expressed as RSS.
354 For improved clarity, both axes are presented on log scales (for this, the negative RSS values of 4 samples
355 of the cohort on the right had to be manually converted to a value of 0.5).
356 Colors are used to represent the HAT results: red: positive, blue: negative, yellow: partially positive
357 hemagglutination, black: false positive, i.e. samples for which hemagglutination also occurred with the
358 IH4 nanobody not coupled to the RBD domain.

The results of the first cohort (Figure 2A) show a clear-cut dichotomy in the distribution of the points, with two well separated clouds: one of blue points falling in the lower left quadrant, and one of red points in the upper right one. In other words, for this cohort of sera collected either from hospitalized Covid-19 patients or dating from before the pandemic for the negative controls, the three tests are in almost perfect agreement for the discrimination between positives and negatives, with just one yellow point in the lower right quadrant, i.e. positive for the Jurkat-S&R-flow test, showing only partial hemagglutination, but the signal for the RBD-ELISA test falling slightly below the threshold of 1 set by the manufacturer, suggesting that the anti-viral serological response of this subject was probably focused on regions of the spike protein outside of the RBD domain.

Of note, partial hemagglutination was also recorded for two other samples which were negative for the two other tests. Those two samples were from a group of 38 patients hospitalized for Covid-19, but for whom the blood had been collected less than 14 days after the PCR diagnostic. This observation is in line with our previous observation that the HAT test may be particularly performant for the detection of early serological responses, probably because of a higher hemagglutinating capacity of IgMs (Townsend et al., 2021). Incidentally, in this same group of 'early' PCR-positive Covid patients, there were also 4 other samples which were negative for all three tests (see tables of data provided as supplementary material).

The results of the second cohort, which comprised a few Covid patients, but also a large proportion of blood samples randomly picked among those from patients hospitalized for conditions unrelated to Covid-19, yielded a much less clear picture than the first one. As can be seen on Figure 2B, many of the dots for this cohort occupy a more intermediate position between the two clouds of clearly positive and clearly negative samples. In the upper right quadrant, one notices a relatively high proportion of blue and yellow spots, i.e. of HAT negative or partial samples in the set which were positive with both the RBD-ELISA and Jurkat-S&R-flow tests, albeit in the lower left part of the quadrant, i.e. rather weakly.

On the other hand, there are also a handful of samples in the lower left quadrant for which partial or full hemagglutination was detected, which may correspond to early serological responses. There are also a few blue dots in the upper left and lower right quadrant, thus corresponding to samples being positive only either with the RBD ELISA or the Jurkat-S&R-flow test. According to previous work, the sera which react weakly on the full length spike protein expressed at the surface of Jurkat cells are most likely due to cross-reactivities with the S2 domain of other coronaviruses (Khan et al., 2020; Ng et al., 2020).

One additional conclusion that can be drawn from the comparison of the results of the RBD-ELISA with those of the Jurkat-S&R-flow test is that, whilst the two methods show similar sensitivities, the ELISA signals tend to saturate very rapidly, and are thus much less dynamic that those obtained by flow cytometry.

402 ***Examples of possible uses of the Jurkat-flow test***
403
404 A further advantage of the Jurkat-S&R-flow test compared to the commercial RBD-ELISA we
405 used for this study is that it only requires 1 µL of plasma or serum, compared to 100 µL for the
406 ELISA, which makes it possible to perform on small volumes of capillary blood collected by finger
407 prick.
408
409 As a proof of concept that this was doable and useful, we used capillary blood which one of
410 the authors collected by pricking his finger at various intervals to document the time course of
411 his serological response after vaccination, and the results are shown in panel A of Figure 3. One
412 somewhat surprising finding was with the low levels of IgM recorded, which may in part be
413 explained by the fact that, as a rule, anti-IgM secondary antibodies tend not to work as well as
414 those against the other isotypes. One should note, however, that, with the same anti-IgM
415 secondary reagent, signals of the same order of magnitude were found for IgG and IgM with the
416 20/130 reference serum (Figure 1), in agreement with the activity documented by flow
417 cytometry in the WHO report by the Expert Committee on Biological Standardization
418 (Mattiuzzo et al., 2020). Of note, sizeable IgM staining was also seen in several other samples of
419 the cohort (Table S1). The observation that the signals obtained with an anti-IgG reagent are
420 similar, and even often a bit higher to those obtained with the pan-reactive anti-IgGAM is
421 something which we tend to find in most samples (Table S1), and which had already been
422 underlined by Grzelak et al. in the context of the S-flow test (Grzelak et al., 2020).
423
424 The capacity of the SARS-CoV-2 virus to infect primates, hamsters or ferrets has provided very
425 useful animal models to understand the physiopathology of Covid-19, whilst its capacity to infect
426 domestic pets such as cats and dogs does raise concerns about the transmissions of the virus
427 back to humans, as well as about the problem of animal reservoirs from which it will be very
428 difficult to eradicate the virus. Whilst scores of commercial and lab-made methods have been
429 described to follow human serological responses to the virus, there is a remarkable paucity of
430 tests available today applicable to animals. Since all it would take to adapt the Jurkat-S&R-flow
431 test to animals would be to use different species-specific secondary antibodies, we explored
432 whether this would work for mice, cats, dogs and hamsters.
433

Figure 3

A

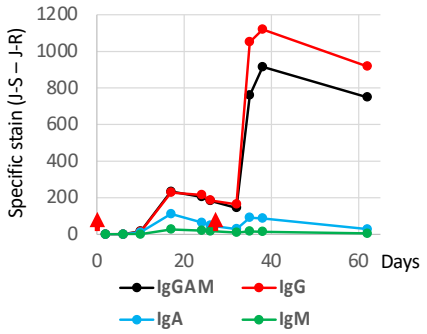

B

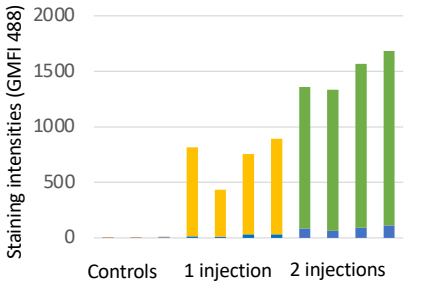

C

Sera from exposed Cats					Sera from exposed Dogs				
Sample ID	GMFI J-S	GMFI J-R	Specific stain	Neutr. titers	Sample ID	GMFI J-S	GMFI J-R	Specific stain	Neutralisation titers
neg cont	2.06	1.87	0.19		neg cont	1.93	1.85	0.08	
PNRA	15.4	12.5	2.9	-	GMLX	25.9	14	11.9	-
VK8X	15.7	9.04	6.66	-	KDEJ	34.6	19.8	14.8	-
MPP5	18	10.6	7.4	-	ZVJX	38.8	23.7	15.1	-
NATW	64.5	51.7	12.8	-	4USK	50.1	32.5	17.6	**1:100**
XEPP	55	36.2	18.8	-	DP5K	44.6	20.7	23.9	-
20-059	57.4	14.3	43.1	-	0006	54.1	29.7	24.4	-
79UQ	71.7	25.8	45.9	**1:400**	XXHT	55.6	13.4	42.2	**1:200**
NP3W	73.6	15.2	58.4	**1:200**	RUML	64.4	10.3	54.1	**1:200**
66JQ	642	30.6	611.4	**>1:1280***	BTFP	87.9	9.72	78.18	**1:100**
AMGT	679	47.6	631.4	**1:100**	KJY8	136	9.82	126.18	**1:200**
GTVJ	730	24.3	705.7	**1:400**	CSSL	246	6.24	239.76	**1:200**

D

	Analysis of live Jurkat cells	Analysis of fixed Jurkat cells
Sera from control hamsters	0.34	0.17
	2.59	2.13
	0.03	0
	-0.21	-0.19
	0.21	0.09
	0.71	0.46
Sera from hamsters after SARS-CoV-2 infection	1122.55	745.41
	1216.53	1076.28
	761.5	669.28
	1183.32	822.22
	725.43	708.31
	608.43	591.25

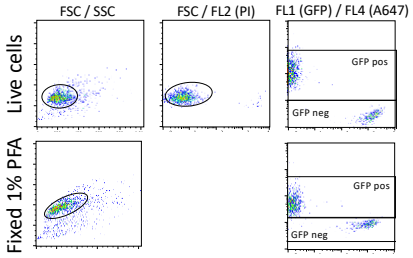

Figure 3: Various examples of the possible uses of the Jurkat-flow test

Panel A: Monitoring serological responses in humans

The Jurkat-S&R-flow test was used to follow the serological response of an individual during the course of his vaccination (red arrows: first injection on day 0 and boost on day 27), with isotyping using specific secondary reagents performed as described in the M&M section. Y axis: Specific staining (GMFI J-S – GMFI J-R)

Panel B: The Jurkat-S&R-flow test can be used to follow Ig responses in mice.

Sera from three groups of mice having been immunized either once, twice or not by intra-peritoneal injection of inactivated SARS-CoV-2 virus were analyzed with the Jurkat-S&R-flow test, using an anti-mouse Ig secondary antibody. Y axis: GMFI on Jurkat-R (blue columns), on Jurkat-S (top of green columns), The specific signals correspond to the yellow or green portions (GMFI J-S – GMFI J-R).

Panel C: In cats and dogs, the results of the Jurkat-S&R-flow test correlate with those of sero-neutralization titers.

Panels of sera from cats and dogs whose owners had recovered from symptomatic Covid-19, and which had been found to be either positive or negative by sero-neutralization assays, were used to perform the Jurkat-S&R-flow test, using the corresponding secondary antibodies. Negative controls were performed with secondary antibodies only, and no serum added during the primary incubation. Specific stain = GMFI J-S – GMFI J-R. *: the higher SN titers shown for the cat serum 66JQ was obtained on a different day from all the others.

Panel D: Monitoring of antiviral serological responses in Hamsters with the Jurkat-S&G-flow test

For this experiment, we used sera from 6 hamsters which had been experimentally infected with the UCN1 strain of SARS-CoV-2 15 days earlier, as well as 6 uninfected controls. Since we had an anti-hamster Ig secondary antibody conjugated to alexa 647, we used an S&G version of the test, with Jurkat cells expressing GFP as negative control, and propidium iodide to gate out dead cells (see M&M). As can be seen on the right side of the panel, in this configuration, no compensation was required, and separating the Jurkat-S test cells from the Jurkat-G control cells could be performed with simple square gates. And although the GFP signal was reduced after fixation of the cells in PFA for 24 hours analysis of cells was still possible with the FACScalibur, with almost no loss of the alexa 647 signal.

First, we used sera of mice which had been immunized once or twice with inactivated SARS-CoV-2 virus injected intra-peritoneally. As can be seen on panel B of Figure 3, whilst the sera of control mice did not react significantly with Jurkat cells, those of immunized mice showed strong specific reactions against the spike protein, which were even higher in those having received two injections. Of note, the reactions against the Jurkat-R cells also went up in correlation with the injections, albeit to a much lesser degree than against the S protein. This is presumably due to the fact that the preparations of inactivated virus used for the immunizations probably contained some bovine proteins from the serum used in the tissue culture medium that would have the capacity to bind to the surface of the Jurkat cells, such as, for example, bovine beta-2-microglobulin binding to human MHC class I molecules. The Jurkat-S&R-flow method therefore seems to work very satisfactorily in mice, and since it requires only a few µL of blood, it is well suited to follow serological responses over time.

We then turned our attention to cats and dogs, which have both been shown to be susceptible to infections by the SARS-CoV-2 virus (Bessière et al., 2021a; Chen, 2020; Dróżdż et al., 2021; Sit et al., 2020), but for which one of the only reliable means to test for the presence of a serological response is to perform sero-neutralization experiments, which are both cumbersome and require access to BSL-3 facilities. For our exploratory experiments, we simply used sets of sera collected from 11 cats and 11 dogs whose owners had had symptomatic Covid-19 infections, and on which sero-neutralization experiments tests had been performed. To use the Jurkat-S&R-flow test on these, the test was adapted by simply using the appropriate secondary antibodies. As can be seen on panel C of Figure 3, we found a very good correlation between the levels of specific staining of Jurkat-S cells and the neutralization titers of the same sera. Whilst those are very preliminary observations which will need to be strengthened by many more samples, and in particular with samples collected before the Covid-19 pandemic as negative controls, those results show that the Jurkat-S&R-flow test can clearly be used to evaluate the levels of antibodies against the S protein of the SARS-CoV-2 virus in cats and dogs.

Finally, we turned our attention to hamsters, which are susceptible to infection by SARS-CoV-2, and have been a very useful animal model to study the physiopathology of the infection. For this, we made use of a panel of sera from hamsters which had been used in a previous study (Bessière et al., 2021b). Because we had some anti-hamster Ig conjugated to the Alexa -647 fluorochrome at our disposal, we took this opportunity to test the possibility of adapting the Jurkat-S&R-flow test to a Jurkat-S&G-flow test, i.e. using Jurkat cells expressing GFP rather than mCherry as the internal negative control. As can be seen on panel D of figure 3, the sera from the hamsters that had been experimentally inoculated with the SARS-CoV-2 virus two weeks earlier all harbored very high levels of antibodies against the virus, whilst no signal was detected with the sera from control animals. Of note, with the S&G version of the test, i.e. using GFP-expressing Jurkat cells as negative control and a secondary antibody conjugated to alexa-647, since the two signals were collected on the separate green and red laser lines of the FACScalibur, the situation was similar to when we analyzed the Jurkat-S&R-flow test on a Fortessa flow cytometer: gating to separate the test from the control cells was achieved with simple rectangular gates, and although fixation in PFA resulted in a twofold reduction of the GFP fluorescent signal, and the auto-fluorescence of the Jurkat-S cells increased about threefold, the efficient triggering of GFP by the 488 nm laser meant that the test and control populations could

510 still be separated and analyzed after fixation, albeit staining with propidium iodide could no
511 longer be used to gate out dead cells.
512
513 ## Concluding remarks and perspectives
514
515 Given its versatility, flexibility and affordability, we believe that the Jurkat-S&R-flow or Jurkat-
516 S&G-flow assays could prove useful for many research scientists wanting to measure serological
517 responses directed towards the spike protein of the SARS-CoV-2 virus, either in humans, or in
518 animals, but who would not have either the financial means to purchase commercial plate-based
519 assays such as ELISA or CLIA, or access to the sizeable amounts of recombinant proteins required
520 to set those up in-house. The Jurkat-flow tests could be performed by any laboratory with access
521 to tissue culture and to a flow cytometer, at a cost of roughly 10 cents per sample (see M&M for
522 calculation). It is thus much cheaper than commercial ELISAs, which cost around 500 € per plate
523 of 90 samples. And the Jurkat-flow test is also completely modular, i.e. each test only comprises
524 the number of samples required, contrary to plate-based assays for which it is rather difficult not
525 to use up a whole plate every time.
526
527 Several reports have already highlighted that using flow-cytometry for the detection of
528 antibodies binding to the S protein expressed at the surface of cells tends to perform better than
529 plate-based assays which use immobilized recombinant proteins (Egia-
530 Mendikute et al., 2021; Goh et al., 2021; Grzelak et al., 2020; Hambach et al., 2021; Horndler et a
531 l., 2021; Lapuente et al., 2021; Ng et al., 2020; Piñero et al., 2021). This is most likely related to
532 the fact that many antibodies will be binding to conformational epitopes, which will only be
533 found on the naturally expressed and properly folded spike protein. In this regard, the capacity of
534 the S protein to undergo structural fluctuations, particularly at the level of the RBD domain
535 which can be in either an open/up or closed/down conformation, has been shown to influence
536 the binding-capacity of various antibodies
537 (Barnes et al., 2020; Dejnirattisai et al., 2021; Harvey et al., 2021b; Huang et al., 2021; Piccoli et al
538 ., 2020; Robbiani et al., 2020; Zhou et al., 2020). This is supported by the results shown in Figure
539 S2, i.e. that, for most samples, we found that incubation at room temperature resulted in a
540 sizeable increase in the amounts of antibodies binding to the spike-expressing cells, suggesting
541 that, at the surface of live cells, the capacity of the spike protein to fluctuate between various
542 conformations will expose different epitopes, and allow the binding of more antibodies.
543
544 One striking aspect of the results shown on Figure 2 is in the difference of performance of the
545 tests between the two cohorts of samples tested. On the one hand, nearly perfect scores were
546 obtained for all three tests on a cohort of sera comprised either of control samples collected
547 before 2019, or of positive sera from PCR-positive Covid-19 patients. On the other hand, the
548 situation was much less clear-cut for the cohort comprising blood samples picked more or less
549 randomly and blindly among those available as left-overs from the hematology department and
550 was, therefore, more akin to a 'real' population. For this second cohort, an additional
551 confounding factor may have been that, since all the samples were from hospitalized patients,
552 some sera may have been poly-reactive due to inflammatory pathologies unrelated to Covid-19.
553
554 All in all, this difference between the two cohorts is reminiscent of the common observation
555 that the performances of clinical tests are often much lower on real populations than those

556 obtained by the manufacturers on very carefully controlled and standardized populations. Our
557 results indeed bring support to the view that the performance of any given serological test will
558 be entirely dependent on the set of samples used to measure it: whilst it is relatively easy to
559 reach an almost perfect score on a cohort comprised only of highly positive and completely
560 negative samples such as the one used for Figure 2A, the situation becomes much less clear
561 when using a set of samples more closely resembling the general population, in which the
562 positive or negative nature of many samples will remain uncertain, and from which it would thus
563 seem futile to try to make precise calculations of sensitivity and specificity. This being said,
564 performing several tests in parallel on such cohorts is very useful to compare the performance of
565 those tests with one another.
566
567 Several recent reports have underlined the correlation between the serological levels of
568 neutralizing antibodies, which are mostly directed against the RBD, and the degree of protection
569 against becoming infected, or re-infected, by the SARS-Cov-2 virus (Feng et al., 2021; Garcia-
570 Beltran et al., 2021; Khoury et al., 2021). Low levels of antibodies are often found in convalescent
571 subjects following asymptomatic infections, and Kalamadasa and colleagues have shown that,
572 whilst HAT sensitivity in such individuals can be as low as 50 %, HAT results are strongly
573 correlated with the seroneutralisation activity in those samples (Kamaladasa et al., 2021). Over
574 the coming months and years, antibodies levels will progressively decrease in both vaccinated
575 and convalescent people, and one of the crucial questions will be that of when to start planning
576 to administer vaccine boosts. Levels of neutralizing antibodies will certainly evolve very
577 differently in different individuals, and an additional difficult aspect will be to define rules for the
578 administration of vaccine boosts, and whether those should be defined as a general rule (e.g. so
579 many months after the initial vaccination), or individually, based on the monitoring the levels of
580 neutralizing antibodies. For such an individually-based approach, HAT would seem to be a
581 particularly appropriate solution since it is a very simple and cheap test based on the binding of
582 antibodies to the RBD domain (Joly and Maurel Ribes, 2022; Townsend et al., 2021), which are
583 those with neutralizing activity. Furthermore, because the only reagent in HAT simply comprises
584 small amounts of soluble IH4-RBD protein, the hemagglutination test can be very easily adapted
585 to detect antibodies binding to variant forms of the virus (Jayathilaka et al., 2021).
586
587 Whilst HAT is not as sensitive as an anti-RBD ELISA or the Jurkat-S&R-flow test, this relatively
588 low sensitivity may not really be a problem for using HAT to help decide when to revaccinate
589 people since low levels of antibodies are unlikely to be fully protective. By performing titrations,
590 the HAT assay can also provide a quantitative assessment of the levels of circulating antibodies,
591 which have been shown to correlate strongly with sero-neutralisation titers
592 (Lamikanra et al., 2021). In the initial version of HAT, however, such a quantification can only be
593 performed in a laboratory environment because it requires separation of the plasma or serum
594 from the red blood cells. Making use of the Jurkat-S&R-flow test as a reference, we have been
595 able to develop an adapted version of HAT called HAT-field, which can be performed pretty much
596 anywhere, with no specialized equipment, and can provide a quantitative evaluation of the levels
597 of antibodies in a single step (Joly and Maurel Ribes, 2022).

598 **Detailed Contributions**

599

600 **Authors**

Name	First name	ORCID	contributions
Maurel Ribes	Agnes	0000-0002-7560-9502	Collected and anonymized blood samples; scored HAT tests, corrected the manuscript
Bessière	Pierre	0000-0001-5657-0027	Provided hamster, cat and dog sera; performed SN; helped perform FACS assays, corrected the manuscript
Guéry	Jean Charles	0000-0003-4499-3270	Provided immunized mouse sera; corrected the manuscript
Joly Featherstone	Eloise	0000-0001-9077-359X	Scored HAT tests
Bruel	Timothée	0000-0002-3952-4261	Provided Jurkat-R and -S cells; corrected the manuscript
Robinot	Rémy	0000-0002-3651-0171	Transduced, selected and grew Jurkat cells
Schwartz	Olivier	0000-0002-0729-1475	Provided Jurkat-R and -S cells
Volmer	Romain	0000-0003-1591-3251	Provided hamster sera
Abravanel	Florence	0000-0002-1753-1065	Provided cohort of sera and ELISA kits
Izopet	Jacques	0000-0002-8462-3234	Provided cohort of sera and ELISA kits; made suggestions for the manuscript
Joly	Etienne	0000-0002-7264-2681	Designed and funded the study; Performed the experiments; Wrote the paper.

601

602 **Other contributors**

Townsend	Alain	Designed the IH4-RBD reagent and funded its production
Tiong	Tan	Produced the IH4-RBD reagent
Rijal	Pramilla	Produced the IH4-RBD reagent
Buchrieser	Julian	Generated lentiviral vectors
Porrot	Françoise	Grew Jurkat cells
Featherstone	Carol	Copy edited parts of the manuscript

603

604 ## Acknowledgements

605

606 The authors are extremely grateful to Alain Townsend, Tiong Kit Tan, Pramila Rijal, Julian
607 Buchrieser and Françoise Porrot, who contributed the various materials detailed in the above
608 table, and to Carol Featherstone for copy editing the manuscript. They also gratefully
609 acknowledge the contributions of Marianne Navarra, for her help in setting up the agreement
610 with the hospital; Miriam Pinilla, Karin Santoni and Etienne Meunier for the gift of Topro-3 and
611 for performing the Mycoplasma tests; Emmanuelle Naser and Pénélope Viana from the IPBS flow
612 cytometry facility for their assistance, and the very helpful staff of the Toulouse EFS.
613 Funding: The first part of this project was funded by a private donation. The second part was
614 funded by the ANR grant HAT-field to EJ.

615 ## Materials and Methods
616
617 ### Reagents
618
619 Polyclonal anti-human and anti-mouse Igs secondary antibodies, all conjugated to Alexa-488,
620 were from Jackson laboratories, and purchased from Ozyme (France) . Refs: anti-human Ig-GAM:
621 109-545-064, -G: 109-545-003, -A: 109-54-011, -M: 109-545-129; anti-mouse Ig-G: 115-545-003
622
623 Anti-cat IgG (F4262) and anti-dog IgG (F7884) secondary antibodies, both conjugated to FITC,
624 were obtained from Sigma.
625
626 Anti-hamster IgG conjugated to Alexa 647 was obtained from Invitrogen (A-21451)
627
628 Anti RBD monoclonal antibodies: FI3A (site 1) and FD-11A (site 3) (Huang et al., 2021); C121
629 (site 2) (Robbiani et al., 2020); CR3022 (site 4) (ter Meulen et al., 2006); EY6A (site 4)
630 (Zhou et al., 2020). All those were obtained using antibody-expression plasmids, as previously
631 described (Townsend et al., 2021).
632
633 The 20/130 WHO reference serum was obtained from the NIBSC (Potters Bar, UK)
634
635 BSA Fraction V was obtained from Sigma (ref A8022).
636
637 PBS and tissue culture media were obtained from Gibco.
638
639 **Generation of Jurkat-S, Jurkat-R and Jurkat-G cell lines**
640 All three cell lines were obtained by means of lentiviral transduction.
641 pLV-EF1a-SARS-CoV-2-S-IRES-Puro was created by cloning a codon-optimized version of the
642 SARS-CoV-2 S gene (GenBank: QHD43416.1) into the pLV-EF1a-IRES-Puro backbone (Addgene
643 plasmid # 85132 ; http://n2t.net/addgene:85132 ; RRID:Addgene_85132) using BamHI and EcoRI
644 sites.
645 The lentiviral vector for the expression of mCherry was obtained by replacing the GFP
646 sequence of GFP by that of mCherry in the pCDH-EF1α-MCS*-T2A-GFP plasmid
647 (https://systembio.com/shop/pcdh-ef1α-mcs-t2a-gfp-cdna-single-promoter-cloning-and-
648 expression-lentivector/)
649 Lentiviral infectious supernatants were obtained after transient transfection of HEK cells with
650 pLV- or pCDH-derived vectors, together with the packaging R8-2, and VSV-G plasmids.
651 Supernatant was harvested 24h and 48h post transfection, passed through a 45 µm filter and
652 stored in aliquots at -80°C. For the transduction of Jurkat cells, those were distributed in a 6 well
653 plate at 1.5. 10^6 cell per well, in a volume of 500 µL of tissue cuture medium (RPMI, 10 % FCS, 1%
654 PS, 2% Hepes), and 20 µL of the infectious supernatants were added, as well as 5 µL of Lentiblast
655 premium (OZBiosciences). The plate was then spun at 1000g for 60 min at 32°C, before adding
656 2.5 ml of tissue culture medium and returning the plate to the 37°C incubator. Selection with
657 puromycin was then performed at a concentration of 10µg/mL.
658 After a few days, the population of Jurkat cells thus obtained was stained for flow cytometry
659 analysis using a highly reactive serum from a covid-19 patient, and it was found that most cells
660 expressed the S protein, but at low to intermediate levels. To obtain a population that would

661 express higher levels, we submitted this population to three successive rounds of sterile cell
662 sorting using a FACSAria Fusion cell sorter (Beckton Dickinson), selecting each time the 5 % of
663 cells with the brightest staining. Cells were placed back in culture and reamplified after each
664 round of selection. At the time of the second round of sorting, the cell sorter was also used for
665 single cell cloning, but all of the dozen clones obtained by this means showed lower expression
666 that the sorted population. The expression of the S protein in the population of Jurkat cells
667 obtained after these three rounds of sorting was found to remain expressed in all cells, and at
668 similar levels, for more than 50 successive passages, over many weeks of continuous cell culture.
669
670 The Jurkat-R cells were obtained by successive transduction with the pCDH-GFP lentiviral
671 vector described above, then with the empty pLV lentiviral vector, followed by selection with
672 Puromycin at 10µg/mL. FACS analysis revealed that the mCherry fluorescent protein was
673 expressed in 100 % of the cells of the population thus obtained, which therefore did not need to
674 undergo any cell sorting.
675
676 After the initial selection process, both the Jurkat-S and Jurkat-R cell line were maintained in
677 RPMI, 10 % FCS, 2 mM Glutamine, 1% PS and Puromycin at 2.5 µg/mL. The Jurkat-S and Jurkat-R
678 cell lines were both checked for the absence of mycoplasma contamination using the HEK blue
679 hTLR2 kit (Invivogen, Toulouse, France).
680
681 The Jurkat-G cell line was obtained by transduction with the Trip-GFP lentiviral vector
682 (Zennou et al., 2000). Cell sorting was used to bring the 90% of the Jurkat cells that were
683 expressing GFP after the initial transduction to 100 %. The cells were then kept in culture for
684 several dozen passages in standard tissue culture medium with no detectable loss of GFP
685 expression.
686
687 **FACS staining**
688 Before experiments, cells in the cultures of both Jurkat-S and Jurkat-R cell lines were counted,
689 and sufficient numbers harvested to have a bit more than 10^5 cells of each per sample to be
690 tested. Cells from both cell lines were then spun, and resuspended in their own tissue culture
691 medium at a concentration of 2.2 10^6 cells/ mL before pooling equal volumes of the two.
692 Plasmas or sera to be tested were diluted 1/10, either in PBS or in PFN (PBS / 2% FCS / 200
693 mg/L sodium azide). 10 µL of these 1/10 dilutions were then placed in U-bottom 96 well plates,
694 before adding 90 ul per well of the Jurkat-S&R mix.
695 The plates were then incubated for 30 minutes at room temperature before placing them on
696 ice for a further 30 minutes. As can be seen on the supplementary Figure 2, we have found that
697 this initial incubation at room temperature results in a marked increase of the staining signals for
698 most antibodies.
699 All subsequent steps were carried out in the cold, with plates and washing buffers kept on ice.
700 After the primary staining, samples were then washed in PFN, with resuspending the cells by
701 tapping the plate after each centrifugation, and before adding the next wash. After 3 washes,
702 one drop (i.e. ca. 30 ul) of secondary fluorescent antibody diluted 1/200 in PFN was added to
703 each well, and the cells resuspended by gentle shaking of the plates.
704 After an incubation of 60 min on ice, samples were washed two more times with cold PFN
705 before transferring the samples to acquisition tubes in a final volume of 300 ul PFN containing 30
706 nM TO-PRO™-3 Iodide (Thermo Fischer Scientific, ref T3605).

707 This protocol was used for staining with just one pan-specific secondary antibody, i.e. for most
708 of the samples of this study. For specific isotyping, i.e. for staining separately with either anti-IgG,
709 -IgA or -IgM, as well as the pan-specific anti-Ig-GAM secondary antibody, we used double the
710 quantities of cells and of serum or plasma for the primary step, and split the samples into 4 wells
711 after the second wash, before proceeding to the subsequent steps as for the standard protocol.
712 The vast majority of the experiments for this study were analyzed on a FACScalibur flow
713 cytometer controlled by the Cellquest pro software (Version 5.2, Beckton Dickinson), using the
714 FL1 channel for Alexa-488 or FITC, the FL3 channel for m-Cherry, and the FL4 channel (with the
715 633 nm laser) for live gating with the TO-PRO™-3 live stain.
716 For the samples shown on supplementary Figure 1, double quantities were used (as for
717 isotyping) so that the same samples could also be acquired on a Fortessa flow cytometer,
718 controlled by the Diva software (Beckton Dickinson). After the samples had been run on both
719 machines, an equivalent volume of PBS with 2% formaldehyde what added to what was left in
720 the tubes, and those were stored at 4°C for 4 days before they were once again analyzed on both
721 machines.
722 Post-acquisition analysis of all the samples was performed using the Flowjo software (version
723 10.7.1)
724 For the Jurkat-S&G-flow test, Jurkat-R cells were replaced by Jurkat-G cells, we used a
725 secondary antibody conjugated to alexa 647, and TO-PRO™-3 Iodide was replaced by propidium
726 iodide at 2 ug/ml final concentration. The samples were then analyzed on the same FACScalibur
727 flow cytometer, using the FL1 channel for the GFP fluorescence, FL2 for live gating with
728 propidium iodide, and FL4 for the Alexa-647 signals.
729
730 **Cost of the Jurkat-S&R-flow test**
731 The cost per sample of the Jurkat-S&R-flow test lies in large part with the price of the
732 secondary antibodies used. Typically, one vial of secondary antibody costs about 150 € for 1ml,
733 and using 30-50 ul at a 1/200 dilution will provide for at least 5000 samples. The cost of a
734 polyclonal antibody is thus of the order or 3-5 cts per sample.
735 Each sample requires 2.10^5 jurkat cells, which is roughly the amount obtained with 0.5 ml of
736 standard tissue culture medium, which costs around 50 €/L, i.e. 2.5 cts/sample. All in all, if one
737 adds the cost of TC, buffers for the washes and disposable plastics, we estimate that the cost per
738 sample will be of the order of 10 cts.
739 The cost of access to a flow cytometer will be extremely variable between laboratories and
740 institutes. If the cost of access is 20 € per hour, and one runs 200 samples per hour, this will add
741 another 10 cts to the cost per sample.
742
743 **HAT tests**
744 HAT tests were performed using the IH4-RBD reagent diluted at 1 ug/ml in PBN rather than in
745 straight PBS as originally described (Townsend et al., 2021), which results in a slight improvement
746 of the HAT performances, and much improved stability of the IH4-RBD stocks (Joly et al., man in
747 prep.). PBN simply consists of PBS complemented with 1% BSA and 200 mg/L sodium azide. The
748 main role of BSA is to prevent the IH4-RBD reagent from adsorbing onto the plastic of tubes and
749 assay plates, and the azide prevents bacterial and fungal contaminations of the stocks. HAT tests
750 were all performed in V-bottom 96 wells plates (Sarstedt, ref 82 1583).
751 For performing HAT on sera, two tubes of suspension of RBC from an O- donor were prepared
752 at approximately 6µL of packed RBC per ml of PBN. The first tube was used to fill the negative

753 control wells with 90 µL per well. The IH4-RBD reagent was added at 1.1 ug/ml to the second
754 tube of RBC suspension and this was dispensed at 90 µL per test well. Sera to be tested were
755 diluted 1/10 in PBS, and 10 µL of the dilutions were added to a control and a test well.
756 For performing HAT on whole blood samples, which were all leftover clinical samples collected
757 in EDTA tubes (purple tops), 10 µL were diluted with 60 µL of PBS + 5 mM EDTA, and 10 µL of this
758 1/7 dilution were added to each of two wells containing either 90 µL of PBN for the negative
759 controls, or 90 µL of PBN containing 1.1 µg/mL of IH4-RBD reagent for the test wells.
760
761 For both sera and whole blood samples, after 60 minutes incubation at room temperature,
762 the V bottom plates were placed on a homemade light box tilted at an angle of approximately
763 10° from the vertical, and pictures taken with a mobile phone after approximately 20 seconds.
764 In an attempt to increase the sensitivity of the method by detecting partial hemagglutinations,
765 the plates were then returned to a horizontal position for a further two hours, and the procedure
766 of tilting the plate and taking pictures was repeated.
767 As a final step, to ensure that the RBCs in all the 267 blood samples of the second cohort were
768 expressing glycophorin, 30 ul of the monoclonal antibody CR3022 diluted at 200 ng/ml in PBN
769 were added to all samples and resuspended by pipetting with a multichannel pipet. The plates
770 were tilted one more after another 60 minutes, and intense hemagglutination was seen in all 267
771 samples.
772 After transferring all the pictures to computer files, the hemagglutination tests were scored by
773 three independent assessors, of which two were blinded.
774 The scoring system was as follows: A score of 1 was given only to those samples which
775 showed complete hemagglutination after one hour. A score of 0.5 was given to samples which
776 showed either partial hemagglutination after one hour, or partial or complete hemagglutination
777 after the second incubation of 2 hours.
778 This revealed that, whilst there was 100% agreement between the three assessors for the
779 scoring of complete hemagglutination, the scoring of partial hemagglutination proved to be
780 much more subjective and variable, and only those samples which had been scored as partials by
781 all three assessors were finally considered as bona fide partial hemagglutinations.
782
783 **ELISA**
784 The ELISA tests were performed using the WANTAI SARS-CoV-2 Ab ELISA (ref WS-1096),
785 according to the manufacturer's instructions. This commercial kit allows detection of all human
786 antibody isotypes recognizing a recombinant RBD domain of the SARS-Cov-2 virus.
787 The ELISA tests for the cohort of 121 sera were performed in the virology department of the
788 Toulouse hospital, as described previously (Abravanel et al., 2020).
789 The series of ELISA tests for the cohort of 267 plasmas were performed at the IPBS, with the
790 washes being performed by hand rather than by an automated machine, and the 450/625 ODs
791 read by a µQuant plate reader. All the positive samples of this cohort, as well as a set of
792 randomly selected negatives, were submitted to a repeat of the assay, which showed excellent
793 reproducibility.
794
795 **Human samples**
796 Purpan cohort: The collection of 2019 (negative) and SARS-CoV-2 infected (positive) patients
797 was obtained from the laboratory of virology of the Purpan hospital, as previously described
798 (Abravanel et al., 2020).

799 Rangueil Cohort: The samples were routine care residues from random patients, anonymized
800 within 48 hours of collection, regardless of gender or hospitalization reason, collected in the
801 course of a month between the end of January and the end of February 2021. The Covid status
802 (PCR or positive serology) was unknown to the person performing the Jurkat-S&R-flow, ELISA and
803 HAT experiments. Those whole blood samples were kept at room temperature until being used
804 for HAT assays within 24 hours of obtaining them from the hospital. In trial experiments, we had
805 found that such samples could be stored for up to 5 days without any noticeable difference in
806 the performance of the HAT test.
807 After the whole blood samples had been used for HAT assays, the tubes were then spun, and
808 the plasmas harvested into fresh tubes (to which sodium azide was added at a final
809 concentration of 200 ug/ml). Those harvested plasmas were kept at 4°C until they were used to
810 perform the Jurkat-S&R-flow tests and ELISA tests.
811 Capillary blood: one of the authors of this study collected 50 µL of his own blood by finger
812 pricking, using disposable lancets (Sarstedt ref 85.1016) on various days during the course of his
813 vaccination regimen with the Pfizer/BioNTech vaccine. At the time of collection, the blood
814 samples were diluted with 200 µL of PBS + 5mM EDTA (Since whole blood is roughly 50% RBCs
815 and 50% plasma, this 1/5 dilution of the blood actually corresponds to a 1/10 dilution of the
816 plasma). The plasma was then separated from the RBCs after centrifugation, placed in another
817 tube with sodium azide, and stored at 4°C until the day of the assay.
818
819 **Experiments on mouse sera**
820 Virus preparation and inactivation
821 SARS-CoV2 was grown on Vero E6 cells (ATCC) in DMEM (Dutscher) supplemented with
822 100 U/mL penicillin, 100 µg/ml streptomycin (Invitrogen), and 2% heat inactivated fetal bovine
823 serum (Sigma). Viral stocks were propagated in 300 cm^2 flasks (Dutscher) in which 10^3 tissue
824 culture infectious dose 50 ($TCID_{50}$) were inoculated in 100 ml of medium for 3 days at 37°C with
825 5% CO_2. Culture supernatants containing the viral stocks were harvested and inactivated with
826 BPL (Fischer) overnight at 4°C. Virus was then concentrated by ultracentrifugation at 25 000 rpm
827 (for 2 hours at 4°C) on a 20% sucrose cushion in Ultra-Clear centrifuge tubes (SW-32 Ti rotor,
828 Beckman). Pellets were resuspended in PBS, protein concentration was quantified by BCA
829 Protein Assay kit (Pierce). BPL-inactivated SARS-CoV2 stocks at protein concentrations ranging
830 from 1 to 5 µg/µL were stored at -80°C until use.
831 Mouse immunization
832 Mice were injected intra-peritoneally with 15 µg of BPL-SARS-CoV2 in 250 µl of PBS, and then
833 challenged with the same amount at day 62. Mice were euthanized and serum was collected at
834 day 14 post-primary immunization and at day 7 post-secondary challenge. Those experiments
835 were conducted within the scope of the APAFIS licence n° 15236 delivered to Jean Charles Guéry.
836

837
838 **Experiments on Cat and Dog sera**
839 Cats and dogs belonging to owners who developed COVID-19-like symptoms and
840 subsequently tested positive for SARS-CoV-2 infection by RT-qPCR were identified in the frame of
841 a larger study (Bessière *et al.*, manuscript submitted). Blood samples from those animals were
842 collected by veterinary practitioners in dry tubes by standard venipuncture at least one month
843 after the owners' recoveries. After separation from the blood clots by centrifugation, the serum
844 samples were stored frozen at -20°C until the day of the assays. Samples and data collections
845 were conducted according to the guidelines of the Declaration of Helsinki, and approved by the
846 Ethics Committee Sciences et Santé Animale n◦115 (protocol code COVIFEL approved on 1
847 September 2020, registered under SSA_2020_010).
848 Sero-neutralisation assay
849 Serum samples and controls were heat-inactivated at 56 °C for 30 min, serially diluted in
850 DMEM starting at 1:10, mixed with an equal volume of SARS-CoV-2 stock (previously amplified
851 and titrated on Vero-E6 cells and diluted in DMEM to contain 2000 $TCID_{50}$/ml), incubated for 2
852 hours at 37 °C, and 100 µL transferred to tissue-culture 96 well plates plated with 12.000 Vero-E6
853 cells per well the day before the assay, in DMEM complemented with 10% of heat-inactivated
854 fetal bovine serum and 1% of penicillin-streptomycin at 37 °C with 5% of CO2 (medium was
855 removed before adding the virus-serum dilutions). After 60 minutes at 37°C, the virus-serum
856 dilutions were removed before adding DMEM complemented with 2% of heat-inactivated fetal
857 bovine serum and 1% of penicillin-streptomycin. Cells were then incubated for 72 h at 37 °C with
858 5% of CO2. Individual wells were then screened by eye under the microscope for cytopathic
859 effects. Monoclonal anti-SARS-CoV CR3022 antibody (BEI Resources, NIAID, NIH) was used as a
860 positive control. PBS was used as a negative control. Experiments were carried out in a biosafety
861 level 3 facility at the National Veterinary School of Toulouse.
862 Jurkat-S&R-flow test on cat and dog sera
863 For the purpose of the experiment presented in figure 3, which was just intended as a proof
864 of concept that the Jurkat-S&R-flow test could work on cats and dogs, we selected panels of cats
865 and dogs sera which had already been tested by sero-neutralisation so as to have a roughly
866 50/50 distribution of positive and negative samples. The Jurkat-flow test was carried out exactly
867 in the same manner as described for human samples, using each serum sample diluted to 1% v/v
868 to stain 10^5 cells in a final volume of 100 µl, and using the appropriate anti-cat or anti-dog FITC-
869 conjugated secondary antibodies diluted 1/200.
870
871 **Experiments on virally-infected hamsters**
872 Eight week-old female Syrian golden hamsters (*Mesocricetus auratus*, strain RjHan:AURA)
873 from Janviers's breeding Center (Le Genest, St Isle, France) were housed in an animal-biosafety
874 level 3 (A-BSL3), with *ad libitum* access to water and food. Animals were anesthetized with
875 isoflurane and inoculated intranasally with 10^4 $TCID_{50}$ units of UCN1 SARS-CoV-2 strain split in
876 20µL in each nostril. SARS-CoV-2 strain UCN1 was amplified as described previously and used at
877 passage 2 (Bessière et al., 2021b; Monchatre-Leroy et al., 2021). Non-infected animals received
878 the equivalent amount of PBS. Animals were weighted and clinically monitored daily. Six animals
879 from each group were anesthetized and euthanized by exsanguination at 15 dpi. Sera were
880 harvested and aliquots were kept frozen until they were needed for the experiments described
881 here.

The animal experimentation protocols complied with the regulation 2010/63/CE of the European Parliament and of the council of 22 September 2010 on the protection of animals used for scientific purposes. These experiments were approved by the Anses/ENVA/UPEC ethic committee and the French Ministry of Research (Apafis n°24818-2020032710416319).

Ethical statement

All sera from the first cohort, and whole blood samples from the second cohort, were obtained from the Toulouse hospital, where all patients give, by default, their consent for any biological material left over to be used for research purposes after all the clinical tests requested by doctors have been duly completed. Material transfer was done under a signed agreement (CNRS n° 227232, CHU n° 20 427 C). This study was declared and approved by the governing body of the Toulouse University Hospital with the agreement number RnIPH 2021-99, confirming that ethical requirements were fully respected.

Using such materials, we did not really have control over how representative our cohorts may be, but this allowed us to circumvent the very stringent rules set by French laws regarding the use of human materials for research (RIPH, Loi Jardé). Under those rules, setting up a clinical trial involving biological materials of human origin would require many months of administrative procedures and paperwork, as well as several hundreds of thousands of euros, which we did not have access to.

For the same reason, the blood samples for the experiment shown on Figure 3A were collected by one of the authors by simple finger-pricking. He did so on his own free will, without the intervention of anybody else, thus circumventing the need for ethical approval.

Bibliography

Abravanel, F., Miédouge, M., Chapuy-Regaud, S., Mansuy, J.-M., and Izopet, J. (2020). Clinical performance of a rapid test compared to a microplate test to detect total anti SARS-CoV-2 antibodies directed to the spike protein. J. Clin. Virol. *130*, 104528.

Abu-Raddad, L.J., Chemaitelly, H., Coyle, P., Malek, J.A., Ahmed, A.A., Mohamoud, Y.A., Younuskunju, S., Ayoub, H.H., Kanaani, Z.A., Kuwari, E.A., et al. (2021). SARS-CoV-2 reinfection in a cohort of 43,000 antibody-positive individuals followed for up to 35 weeks. MedRxiv.

Adams, E.R., Ainsworth, M., Anand, R., Andersson, M.I., Auckland, K., Baillie, J.K., Barnes, E., Beer, S., Bell, J.I., Berry, T., et al. (2020). Antibody testing for COVID-19: A report from the National COVID Scientific Advisory Panel. Wellcome Open Res. *5*, 139.

Amanat, F., Stadlbauer, D., Strohmeier, S., Nguyen, T.H.O., Chromikova, V., McMahon, M., Jiang, K., Arunkumar, G.A., Jurczyszak, D., Polanco, J., et al. (2020). A serological assay to detect SARS-CoV-2 seroconversion in humans. Nat. Med. *26*, 1033–1036.

Barnes, C.O., Jette, C.A., Abernathy, M.E., Dam, K.-M.A., Esswein, S.R., Gristick, H.B., Malyutin, A.G., Sharaf, N.G., Huey-Tubman, K.E., Lee, Y.E., et al. (2020). SARS-CoV-2 neutralizing antibody structures inform therapeutic strategies. Nature *588*, 682–687.

926 Bessière, P., Fusade-Boyer, M., Walch, M., Lèbre, L., Brun, J., Croville, G., Boullier, S., Cadiergues, M.-C.,
927 and Guérin, J.-L. (2021a). Household Cases Suggest That Cats Belonging to Owners with COVID-19 Have
928 a Limited Role in Virus Transmission. Viruses *13*.

929 Bessière, P., Wasniewski, M., Picard-Meyer, E., Servat, A., Figueroa, T., Foret-Lucas, C., Coggon, A.,
930 Lesellier, S., Boué, F., Cebron, N., et al. (2021b). Intranasal type I interferon treatment is beneficial only
931 when administered before clinical signs onset in the SARS-CoV-2 hamster model. BioRxiv.

932 Chen, H. (2020). Susceptibility of ferrets, cats, dogs, and different domestic animals to SARS-coronavirus-
933 2. BioRxiv.

934 Chen, X., Chen, Z., Azman, A.S., Deng, X., Sun, R., Zhao, Z., Zheng, N., Chen, X., Lu, W., Zhuang, T., et al.
935 (2021). Serological evidence of human infection with SARS-CoV-2: a systematic review and meta-
936 analysis. Lancet Glob. Health *9*, e598–e609.

937 Dejnirattisai, W., Zhou, D., Ginn, H.M., Duyvesteyn, H.M.E., Supasa, P., Case, J.B., Zhao, Y., Walter, T.S.,
938 Mentzer, A.J., Liu, C., et al. (2021). The antigenic anatomy of SARS-CoV-2 receptor binding domain. Cell
939 *184*, 2183-2200.e22.

940 Dortet, L., Ronat, J.-B., Vauloup-Fellous, C., Langendorf, C., Mendels, D.-A., Emeraud, C., Oueslati, S.,
941 Girlich, D., Chauvin, A., Afdjei, A., et al. (2021). Evaluating 10 Commercially Available SARS-CoV-2 Rapid
942 Serological Tests by Use of the STARD (Standards for Reporting of Diagnostic Accuracy Studies)
943 Method. J. Clin. Microbiol. *59*.

944 Dróżdż, M., Krzyżek, P., Dudek, B., Makuch, S., Janczura, A., and Paluch, E. (2021). Current State of
945 Knowledge about Role of Pets in Zoonotic Transmission of SARS-CoV-2. Viruses *13*.

946 Egia-Mendikute, L., Bosch, A., Prieto-Fernández, E., Lee, S.Y., Jiménez-Lasheras, B., García Del Río, A.,
947 Antoñana-Vildosola, A., Bruzzone, C., Bizkarguenaga, M., Embade, N., et al. (2021). Sensitive detection
948 of SARS-CoV-2 seroconversion by flow cytometry reveals the presence of nucleoprotein-reactive
949 antibodies in unexposed individuals. Commun. Biol. *4*, 486.

950 Ertesvåg, N.U., Xiao, J., Zhou, F., Ljostveit, S., Sandnes, H., Jalloh, S.L., Saevik, M., Hansen, L., Madsen, A.,
951 Mohn, K., et al. (2021). A Rapid Antibody Screening Haemagglutination Test for Predicting Immunity to
952 Sars CoV-2 Variants of Concern. Res. Sq.

953 Fani, M., Teimoori, A., and Ghafari, S. (2020). Comparison of the COVID-2019 (SARS-CoV-2) pathogenesis
954 with SARS-CoV and MERS-CoV infections. Future Virol.

955 Farnsworth, C.W., and Anderson, N.W. (2020). SARS-CoV-2 Serology: Much Hype, Little Data. Clin. Chem.
956 *66*, 875–877.

957 Feng, S., Phillips, D.J., White, T., Sayal, H., Aley, P.K., Bibi, S., Dold, C., Fuskova, M., Gilbert, S.C., Hirsch, I.,
958 et al. (2021). Correlates of protection against symptomatic and asymptomatic SARS-CoV-2 infection.
959 MedRxiv.

960 Garcia-Beltran, W.F., Lam, E.C., Astudillo, M.G., Yang, D., Miller, T.E., Feldman, J., Hauser, B.M.,
961 Caradonna, T.M., Clayton, K.L., Nitido, A.D., et al. (2021). COVID-19-neutralizing antibodies predict
962 disease severity and survival. Cell *184*, 476-488.e11.

963 Goh, Y.S., Ng, L.F.P., and Renia, L. (2021). A flow cytometry-based assay for serological detection of anti-
964 spike antibodies in COVID-19 patients. STAR Protocols *2*, 100671.

965 Grzelak, L., Temmam, S., Planchais, C., Demeret, C., Tondeur, L., Huon, C., Guivel-Benhassine, F., Staropoli,
966 I., Chazal, M., Dufloo, J., et al. (2020). A comparison of four serological assays for detecting anti-SARS-
967 CoV-2 antibodies in human serum samples from different populations. Sci. Transl. Med. *12*.

968 Hambach, J., Stähler, T., Eden, T., Wendt, D., Tode, N., Haag, F., Tolosa, E., Altfeld, M., Fathi, A., Dahlke, C.,
969 et al. (2021). A simple, sensitive, and low-cost FACS assay for detecting antibodies against the native
970 SARS-CoV-2 spike protein. Immun. Inflamm. Dis. *9*, 905–917.

971 Harvey, R.A., Rassen, J.A., Kabelac, C.A., Turenne, W., Leonard, S., Klesh, R., Meyer, W.A., Kaufman, H.W.,
972 Anderson, S., Cohen, O., et al. (2021a). Association of SARS-CoV-2 Seropositive Antibody Test With Risk
973 of Future Infection. JAMA Intern. Med. *181*, 672–679.

974 Harvey, W.T., Carabelli, A.M., Jackson, B., Gupta, R.K., Thomson, E.C., Harrison, E.M., Ludden, C., Reeve,
975 R., Rambaut, A., COVID-19 Genomics UK (COG-UK) Consortium, et al. (2021b). SARS-CoV-2 variants,
976 spike mutations and immune escape. Nat. Rev. Microbiol. *19*, 409–424.

977 Hickey, M.J., Valenzuela, N.M., and Reed, E.F. (2016). Alloantibody generation and effector function
978 following sensitization to human leukocyte antigen. Front. Immunol. *7*, 30.

979 Horndler, L., Delgado, P., Abia, D., Balabanov, I., Martínez-Fleta, P., Cornish, G., Llamas, M.A., Serrano-
980 Villar, S., Sánchez-Madrid, F., Fresno, M., et al. (2021). Flow cytometry multiplexed method for the
981 detection of neutralizing human antibodies to the native SARS-CoV-2 spike protein. EMBO Mol. Med.
982 *13*, e13549.

983 Huang, K.-Y.A., Tan, T.K., Chen, T.-H., Huang, C.-G., Harvey, R., Hussain, S., Chen, C.-P., Harding, A., Gilbert-
984 Jaramillo, J., Liu, X., et al. (2021). Breadth and function of antibody response to acute SARS-CoV-2
985 infection in humans. PLoS Pathog. *17*, e1009352.

986 Jayathilaka, D., Jeewandara, C., Gomes, L., Jayadas, T.T.P., Kamaladasa, A., Guruge, D., Darshana, P.,
987 Ranasinghe, T., Abyrathna, I.S., Danasekara, S., et al. (2021). Comparison of kinetics of immune
988 responses to SARS-CoV-2 proteins in individuals with varying severity of infection and following a
989 single dose of the AZD1222. MedRxiv.

990 Jeewandara, C., Kamaladasa, A., Pushpakumara, P.D., Jayathilaka, D., Aberathna, I.S., Danasekara,
991 D.R.S.R., Guruge, D., Ranasinghe, T., Dayarathna, S., Pathmanathan, T., et al. (2021). Immune
992 responses to a single dose of the AZD1222/Covishield vaccine in health care workers. Nat. Commun.
993 *12*, 4617.

994 Jeffery-Smith, A., Iyanger, N., Williams, S.V., Chow, J.Y., Aiano, F., Hoschler, K., Lackenby, A., Ellis, J., Platt,
995 S., Miah, S., et al. (2021). Antibodies to SARS-CoV-2 protect against re-infection during outbreaks in
996 care homes, September and October 2020. Euro Surveill. *26*.

997 Joly, E., and Maurel Ribes, A. (2022). HAT-field: a cheap, robust and quantitative point-of-care serological
998 test for Covid-19. MedRxiv *10.1101/2022.01.14.22268980*.

999 Kamaladasa, A., Gunasekara, B., Jeewandara, C., Jayathilaka, D., Wijewickrama, A., Guruge, D.,
1000 Wijayamuni, R., Tan, T.K., Ogg, G.S., Townsend, A., et al. (2021). Comparison of two assays to detect
1001 IgG antibodies to the receptor binding domain of SARS-CoV-2 as a surrogate marker for assessing
1002 neutralizing antibodies in COVID-19 patients. Int. J. Infect. Dis. *109*, 85–89.

1003 Karahan, G.E., Claas, F.H.J., and Heidt, S. (2020). Pre-existing Alloreactive T and B Cells and Their Possible
1004 Relevance for Pre-transplant Risk Estimation in Kidney Transplant Recipients. Front Med (Lausanne) *7*,
1005 340.

1006 Khan, S., Nakajima, R., Jain, A., de Assis, R.R., Jasinskas, A., Obiero, J.M., Adenaiye, O., Tai, S., Hong, F.,
1007 Milton, D.K., et al. (2020). Analysis of Serologic Cross-Reactivity Between Common Human
1008 Coronaviruses and SARS-CoV-2 Using Coronavirus Antigen Microarray. BioRxiv.

1009 Khoury, D.S., Cromer, D., Reynaldi, A., Schlub, T.E., Wheatley, A.K., Juno, J.A., Subbarao, K., Kent, S.J.,
1010 Triccas, J.A., and Davenport, M.P. (2021). Neutralizing antibody levels are highly predictive of immune
1011 protection from symptomatic SARS-CoV-2 infection. Nat. Med. *27*, 1205–1211.

1012 Koopmans, M., and Haagmans, B. (2020). Assessing the extent of SARS-CoV-2 circulation through
1013 serological studies. Nat. Med. *26*, 1171–1172.

1014 Lamikanra, A., Nguyen, D., Simmonds, P., Williams, S., Bentley, E.M., Rowe, C., Otter, A.D., Brooks, T.,
1015 Gilmour, K., Mai, A., et al. (2021). Comparability of six different immunoassays measuring SARS-CoV-2
1016 antibodies with neutralising antibody levels in convalescent plasma: from utility to prediction.
1017 Transfusion.

1018 Lapuente, D., Maier, C., Irrgang, P., Hübner, J., Peter, A.S., Hoffmann, M., Ensser, A., Ziegler, K., Winkler,
1019 T.H., Birkholz, T., et al. (2021). Rapid response flow cytometric assay for the detection of antibody
1020 responses to SARS-CoV-2. Eur. J. Clin. Microbiol. Infect. Dis. *40*, 751–759.

1021 Letizia, A.G., Ge, Y., Vangeti, S., Goforth, C., Weir, D.L., Kuzmina, N.A., Chen, H.W., Ewing, D.F., Soares-
1022 Schanoski, A., George, M.-C., et al. (2021). SARS-CoV-2 Seropositivity and Subsequent Infection Risk in
1023 Healthy Young Adults: A Prospective Cohort Study. SSRN Journal.

1024 Long, Q.-X., Tang, X.-J., Shi, Q.-L., Li, Q., Deng, H.-J., Yuan, J., Hu, J.-L., Xu, W., Zhang, Y., Lv, F.-J., et al.
1025 (2020). Clinical and immunological assessment of asymptomatic SARS-CoV-2 infections. Nat. Med. *26*,
1026 1200–1204.

1027 Lumley, S.F., O'Donnell, D., Stoesser, N.E., Matthews, P.C., Howarth, A., Hatch, S.B., Marsden, B.D., Cox,
1028 S., James, T., Warren, F., et al. (2021). Antibody Status and Incidence of SARS-CoV-2 Infection in Health
1029 Care Workers. N. Engl. J. Med. *384*, 533–540.

1030 Mattiuzzo, G., Bentley, E.M., Hassal, M., Routley, S., and EXPERT COMMITTEE ON BIOLOGICAL
1031 STANDARDIZATION ON BIOLOGICAL STANDARDIZATION (2020). WHO/BS.2020.2403 Establishment of
1032 the WHO International Standard and Reference Panel for anti-SARS-CoV-2 antibody (World Health
1033 Organization 2020).

1034 ter Meulen, J., van den Brink, E.N., Poon, L.L.M., Marissen, W.E., Leung, C.S.W., Cox, F., Cheung, C.Y.,
1035 Bakker, A.Q., Bogaards, J.A., van Deventer, E., et al. (2006). Human monoclonal antibody combination
1036 against SARS coronavirus: synergy and coverage of escape mutants. PLoS Med. *3*, e237.

1037 Mohit, E., Rostami, Z., and Vahidi, H. (2021). A comparative review of immunoassays for COVID-19
1038 detection. Expert Rev. Clin. Immunol.

1039 Monchatre-Leroy, E., Lesellier, S., Wasniewski, M., Picard-Meyer, E., Richomme, C., Boué, F., Lacôte, S.,
1040 Murri, S., Pulido, C., Vulin, J., et al. (2021). Hamster and ferret experimental infection with intranasal
1041 low dose of a single strain of SARS-CoV-2. J. Gen. Virol. *102*.

1042 Moshe, M., Daunt, A., Flower, B., Simmons, B., Brown, J.C., Frise, R., Penn, R., Kugathasan, R., Petersen, C.,
1043 Stockmann, H., et al. (2021). SARS-CoV-2 lateral flow assays for possible use in national covid-19
1044 seroprevalence surveys (React 2): diagnostic accuracy study. BMJ *372*, n423.

1045 Ng, K.W., Faulkner, N., Cornish, G.H., Rosa, A., Harvey, R., Hussain, S., Ulferts, R., Earl, C., Wrobel, A.G.,
1046 Benton, D.J., et al. (2020). Preexisting and de novo humoral immunity to SARS-CoV-2 in humans.
1047 Science *370*, 1339–1343.

1048 Piccoli, L., Park, Y.-J., Tortorici, M.A., Czudnochowski, N., Walls, A.C., Beltramello, M., Silacci-Fregni, C.,
1049 Pinto, D., Rosen, L.E., Bowen, J.E., et al. (2020). Mapping Neutralizing and Immunodominant Sites on
1050 the SARS-CoV-2 Spike Receptor-Binding Domain by Structure-Guided High-Resolution Serology. Cell
1051 *183*, 1024-1042.e21.

1052 Piñero, P., Marco De La Calle, F.M., Horndler, L., Alarcón, B., Uribe Barrientos, M., Sarmiento, H., and
1053 Tarín, F. (2021). Flow cytometry detection of sustained humoral immune response (IgG + IgA) against
1054 native spike glycoprotein in asymptomatic/mild SARS-CoV-2 infection. Sci. Rep. *11*, 10716.

1055 Robbiani, D.F., Gaebler, C., Muecksch, F., Lorenzi, J.C.C., Wang, Z., Cho, A., Agudelo, M., Barnes, C.O.,
1056 Gazumyan, A., Finkin, S., et al. (2020). Convergent antibody responses to SARS-CoV-2 in convalescent
1057 individuals. Nature *584*, 437–442.

1058 Sit, T.H.C., Brackman, C.J., Ip, S.M., Tam, K.W.S., Law, P.Y.T., To, E.M.W., Yu, V.Y.T., Sims, L.D., Tsang,
1059 D.N.C., Chu, D.K.W., et al. (2020). Infection of dogs with SARS-CoV-2. Nature *586*, 776–778.

1060 Townsend, A., Rijal, P., Xiao, J., Tan, T.K., Huang, K.-Y.A., Schimanski, L., Huo, J., Gupta, N., Rahikainen, R.,
1061 Matthews, P.C., et al. (2021). A haemagglutination test for rapid detection of antibodies to SARS-CoV-
1062 2. Nat. Commun. *12*, 1951.

1063 Wu, Z., Harrich, D., Li, Z., Hu, D., and Li, D. (2021). The unique features of SARS-CoV-2 transmission:
1064 Comparison with SARS-CoV, MERS-CoV and 2009 H1N1 pandemic influenza virus. Rev. Med. Virol. *31*,
1065 e2171.

1066 Zennou, V., Petit, C., Guetard, D., Nerhbass, U., Montagnier, L., and Charneau, P. (2000). HIV-1 genome
1067 nuclear import is mediated by a central DNA flap. Cell *101*, 173–185.

1068 Zhou, D., Duyvesteyn, H.M.E., Chen, C.-P., Huang, C.-G., Chen, T.-H., Shih, S.-R., Lin, Y.-C., Cheng, C.-Y.,
1069 Cheng, S.-H., Huang, Y.-C., et al. (2020). Structural basis for the neutralization of SARS-CoV-2 by an
1070 antibody from a convalescent patient. Nat. Struct. Mol. Biol. *27*, 950–958.
1071

1072

1073 **Supplementary material**

1074

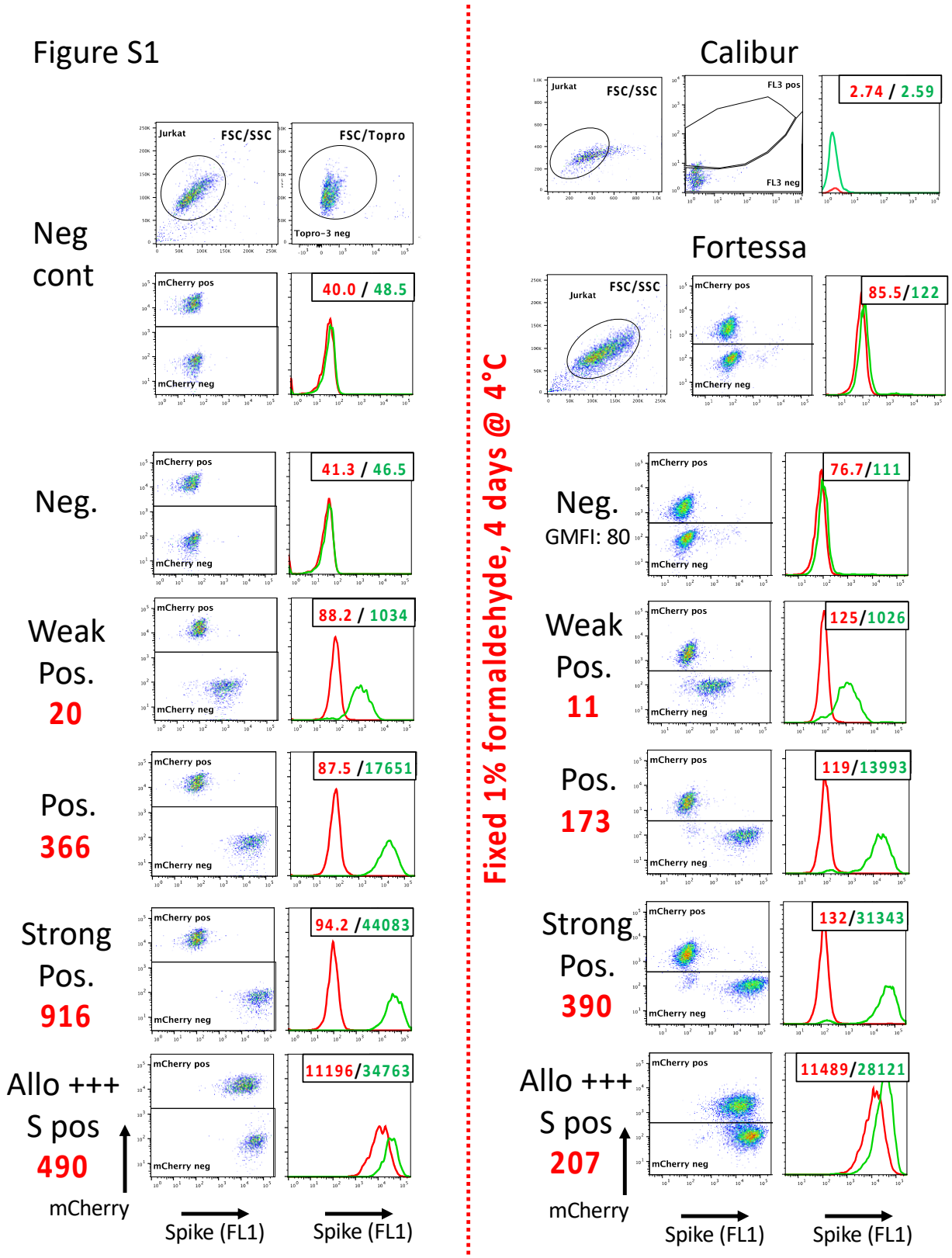

1075

1076

1077 **Figure S1**: Using a flow cytometer with a 561 nm Yellow-Green laser improves the mCherry
1078 signals
1079 The same samples shown on Figure 1 were also analyzed on a Fortessa flow cytometer. The
1080 561 nm yellow-green laser was used for the excitation of the mCherry fluorescent protein, which
1081 led to much brighter signals, and thus to much easier separation of the Jurkat-R (mCherry pos)
1082 and Jurkat-S (mCherry neg) populations than when the samples were acquired on a FACScalibur.
1083 As in figure 1, the numbers in the upper right corners of the histogram overlays plots
1084 correspond to the GMFI of the two histograms (Red: Jurkat-R; Green: Jurkat-S), and the big red
1085 numbers to the left of the plots to the RSS. Of note, although the GMFI values were much higher
1086 on the Fortessa than those recorded on the FACScalibur, the RSS values of the various samples
1087 were all very similar between the two machines.
1088
1089 After the samples had been run on both flow cytometers, those were fixed in 1%
1090 formaldehyde by adding an equal volume of PBS + 2% formaldehyde to the remainder of each
1091 sample. The tubes were then stored à 4°C for 4 days before re-analyzing them on both
1092 cytometers. As can be seen on the right hand side of the figure, the red fluorescence of the
1093 mCherry was still detectable on the Fortessa after this procedure of fixation, despite the intensity
1094 of the signals having dropped by about 7 fold. On the FACScalibur, however, this drop of the
1095 mCherry fluorescent signals precluded the separation of the Jurkat-S from the Jurkat-R cells. If
1096 samples are to be fixed, performing the Jurkat-R&S-flow test will thus require access to a flow
1097 cytometer equipped with a 561 nm Yellow-Green laser. As can be seen on panel D of figure 3, an
1098 alternative is to transform the Jurkat-S&R-flow test into a Jurkat-S&G-flow test, where the
1099 negative control cells express GFP, which is excited at 488 nm, and using secondary antibodies
1100 conjugated to red fluorochromes such as Alexa647, excited by a 633 nm red laser, for the
1101 detection of the primary antibodies.
1102
1103 Of note, in the dot plots of the Positive and Strong Positive fixed samples, faint clouds of FL1
1104 negative cells can be seen in the mCherry neg window. Those presumably correspond to Jurkat-R
1105 cells which were dead before the fixation step, and from which the mCherry had thus leaked out.
1106 When analyzing populations of live cells, such cells are gated out with the To-pro 3 live stain, but
1107 this no longer works for population of fixed cells. This small problem could probably be
1108 circumvented using a fixable dead cell staining dye such as the LIVE/DEAD Fixable Far Red stain
1109 (ThermoFischer L34973).
1110
1111

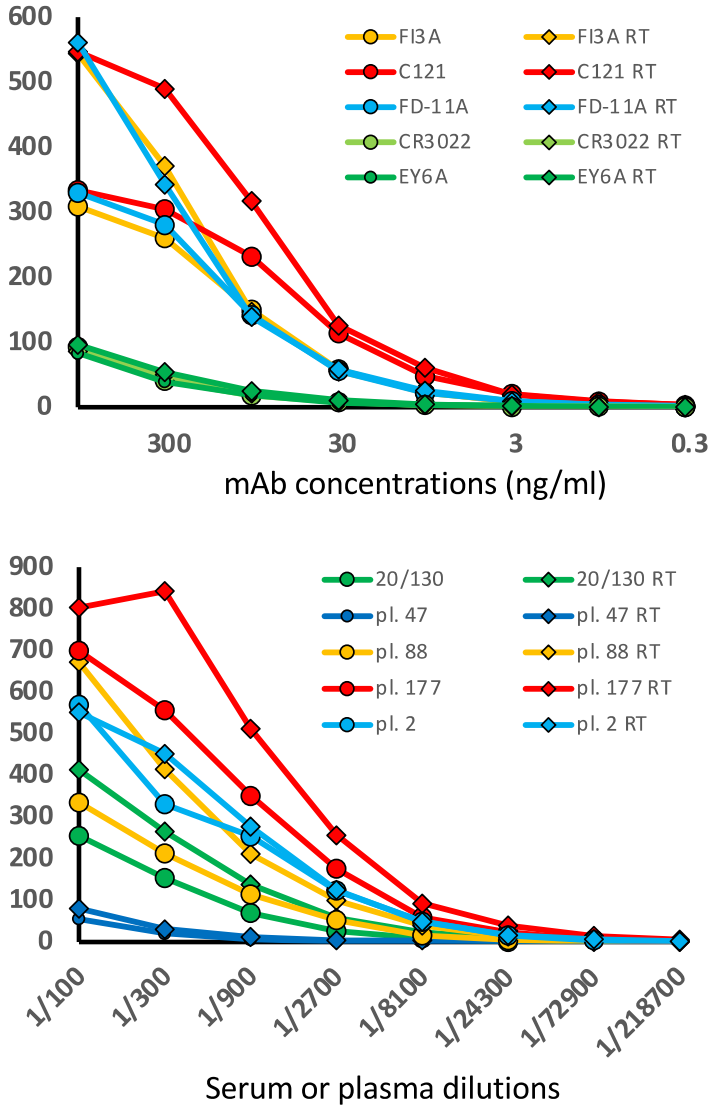

Figure S2: Incubation of the samples at room temperature for the first part of the primary staining step markedly improves the staining signals for most antibodies.

For a large fraction of monoclonal and polyclonal antibodies reacting with the Spike protein expressed at the surface of cells, we have repeatedly observed that a step of incubation at room temperature can result in a marked improvement of the staining signals compared to performing the staining continuously on ice.

For this experiment, we selected a panel of 5 monoclonal antibodies reacting with different sites of the spike RBD domain, a panel of 4 plasmas reacting with various intensities, as well the 20/130 reference serum.

For all the samples, we performed eight steps of 3-fold dilutions, and placed 10 ul of the diluted samples in two parallel U bottom 96 well plates. The first plate was kept at room temperature (RT) whilst the other one was placed on ice. The Jurkat-S&R mix was then added to the wells of the plate at room temperature. The tube was then placed on ice for a few minutes, before distributing the mix in the wells of the second plate. After 30 minutes, the plate which had been sitting at room temperature was also placed on ice, and incubated for another 30 minutes. The rest of the staining procedure was then exactly the same for the two plates, all performed in the cold as described in M&M.

		IgGAM			IgG			IgA			IgM						
	Sample ID	GMFI Jurkat-R	GMFI Jurkat-S	specific stain (J-S - J-R)	GMFI Jurkat-R	GMFI Jurkat-S	specific stain (J-S - J-R)	GMFI Jurkat-R	GMFI Jurkat-S	specific stain (J-S - J-R)	GMFI Jurkat-R	GMFI Jurkat-S	specific stain (J-S - J-R)	G+A+M	Fraction IgG signal	Fraction IgA signal	Fraction IgM signal
	neg	1.87	2.01	0.14	1.95	1.99	0.04	1.79	2.13	0.34	1.89	1.98	0.09	0.47			
Sera	**30/120**	3.19	760	756.81	3.59	763	759.41	2.11	63.2	61.09	2.74	640	637.26	1457.76	0.52	0.04	0.44
	<J14-3	5.1	51.6	46.5	7.47	57.2	49.73	3.08	29.1	26.02	2.55	8.65	6.1	81.85	0.61	0.32	0.07
	<J14-29	4.59	738	733.41	5.16	919	913.84	2.77	122	119.23	2.54	203	200.46	1233.53	0.74	0.10	0.16
	<J14-32	4.71	1692	1687.29	5.25	2350	2344.75	4.01	610	605.99	2.56	402	399.44	3350.18	0.70	0.18	0.12
	<J14-35	4.65	198	193.35	4.82	209	204.18	1.97	52.6	50.63	3.14	13.1	9.96	264.77	0.77	0.19	0.04
	<J14-109	6.52	852	845.48	6.23	1082	1075.77	2.61	179	176.39	4.55	126	121.45	1373.61	0.78	0.13	0.09
	<J14-130	8.7	150	141.3	9.46	151	141.54	3.28	45.7	42.42	5.25	58.1	52.85	236.81	0.60	0.18	0.22
	>J14-40	4.84	54.9	50.06	6.07	54.3	48.23	2.18	12	9.82	2.76	29.1	26.34	84.39	0.57	0.12	0.31
	neg-2213	10.5	33.3	22.8	12.3	43.3	31	3.21	6.58	3.37	6.12	8.77	2.65	37.02	0.84	0.09	0.07
	neg-2649	19.2	41.4	22.2	24.7	56.2	31.5	6.32	9.59	3.27	6.15	9.62	3.47	38.24	0.82	0.09	0.09
Plasmas	**2**	438	1427	989	577	1846	1269	59.4	469	409.6	739	1333	594	2272.60	0.56	0.18	0.26
	18	7.82	84.9	77.08	11.3	101	89.7	2.67	33.4	30.73	4.89	12.7	7.81	128.24	0.70	0.24	0.06
	19	2.02	2.2	0.18	2.07	2.15	0.08	1.82	2.18	0.36	1.83	1.96	0.13	0.57			
	36	4.53	88.7	84.17	5.01	90.2	85.19	2.38	48.5	46.12	3.61	10.4	6.79	138.10	0.62	0.33	0.05
	47	3.47	139	135.53	3.65	141	137.35	2.15	47.1	44.95	2.8	42.2	39.4	221.70	0.62	0.20	0.18
	56	9.03	25.7	16.67	9.48	26.8	17.32	2.56	17.2	14.64	7.16	11.2	4.04	36.00	0.48	0.41	0.11
	57	5.84	25.5	19.66	7.04	26.7	19.66	2.17	8.87	6.7	4.55	13.9	9.35	35.71	0.55	0.19	0.26
	73	3.87	130	126.13	3.61	159	155.39	1.91	4.35	2.44	3.1	4.64	1.54	159.37	0.98	0.02	0.01
	80	2.5	82	79.5	3.07	99.1	96.03	2.06	2.75	0.69	2.21	2.56	0.35	97.07	0.99	0.01	0.00
	83	3.13	1674	1670.87	3.69	1900	1896.31	2.21	542	539.79	2.4	629	626.6	3062.70	0.62	0.18	0.20
	88	3.74	1110	1106.26	4.18	1297	1292.82	2.51	159	156.49	3.03	632	628.97	2078.28	0.62	0.08	0.30
	108	3.53	7.65	4.12	4.22	9.66	5.44	2.08	2.61	0.53	2.6	3.58	0.98	6.95			
	123	54.5	75.6	21.1	51.6	71.4	19.8	4.22	6.14	1.92	43.5	61.1	17.6	39.32	0.62	0.08	0.30
	161	2.91	5.84	2.93	6.17	11.1	4.93	2.08	2.59	0.51	2.09	2.25	0.16	5.60			
	166	101	162	61	109	176	67	27.2	35.3	8.1	46.5	68.9	22.4	97.50	0.69	0.08	0.23
	174	3.11	190	186.89	4.43	228	223.57	2.45	50.1	47.65	2.19	42.3	40.11	311.33	0.72	0.15	0.13
	177	7.9	1945	1937.1	8.04	2303	2294.96	2.32	581	578.68	7.58	699	691.42	3565.06	0.64	0.16	0.19
	227	4.12	77	72.88	5.31	51.4	46.09	2.83	6.19	3.36	3	73.8	70.8	120.25	0.38	0.03	0.59
	232	11	131	120	12.6	169	156.4	6.21	9.13	2.92	4.84	6.83	1.99	161.31	0.97	0.02	0.01
	241	4.11	2411	2406.89	4.61	2860	2855.39	2.6	608	605.4	2.83	47.8	44.97	3505.76	0.81	0.17	0.01
	247	13.8	23.3	9.5	21.6	31.7	10.1	8.87	15.7	6.83	3.5	5.88	2.38	19.31	0.52	0.35	0.12
	253	3.98	28.2	24.22	5.22	33	27.78	2.43	10.7	8.27	2.43	2.9	0.47	36.52	0.76	0.23	0.01
	260	23.2	33.9	10.7	30.8	44.1	13.3	29.4	43	13.6	5.98	7.61	1.63	28.53	0.47	0.48	0.06

Table S1: Example of isotyping performed on a representative set of various serum and plasma samples.

As can be seen on the right hand side portion of the table, comparison of samples from different patients shows that there can be large variations in the proportions of Ig-G,-A and -M. Because polyclonal secondary antibodies will not all react with their targeted primary antibodies with the same efficiency, however, the actuals signals for the various subclasses of antibodies should not be taken as a true reflection of the amounts of each subclass of antibody.
If a more quantitative evaluation was needed, monoclonal secondary antibodies could be used instead of polyclonal reagents, making sure that all those isotypes-specific secondary monoclonal antibodies were being used well above the saturating concentration, and conjugated to similar amounts of the same fluorochrome. This would, however, increase the cost of the procedure considerably.

Peer Review:

The refereeing process of this manuscript was handled by Review Commons (https://www.reviewcommons.org).

We are very grateful to the two referees for their constructive comments and suggestions which have helped improve the quality of our manuscript. This pdf contains de modified version of our manuscript following those suggestions.

The comments from the two referees, and our point by point replies, are provided below.

Reviewer #1 *(Evidence, reproducibility and clarity (Required)):*

Ribes et al developed a FACS-based serological assay to detect antibodies against the SARS-CoV-2 spike protein in various hosts. The authors described an assay that is more sensitive and quantitative, allowing the detection of anti-spike antibodies with just a few ul of blood, and highlighted the potential of the assay as an alternative to commercial ELISA-based assays against SARS-CoV-2 spike protein.

Major concerns

1. On being quantitative analysis - the authors have used 20/130 reference serum from NIBSC as an example in figure 1. How does the RSS of the described assay compare/correlate with the Ab values in WHO standards? This should be included.

Response: We thank the referee for this helpful suggestion, and have now included the information on the IgG BAU in the legend of figure 1, and alluded to the characterisation of the 20/130 by the Expert Committee on Biological Standardization (Mattiuzzo et al., 2020) on lines 410-414 in the main text of the manuscript

2. On sensitivity and specificity - AUC profiles should be performed and included.

Response: If the Jurkat-flow test was intended for clinical use, the precise determination of the sensitivity and specificity of the test would indeed be absolutely essential. As was already mentioned at the end of the introduction, the Jurkat-S&R-flow test is only destined to be used by research laboratories, for research purposes. This has now also been clarified at the end of the abstract : “Whilst the Jurkat-flow test is ill-suited and not intended for clinical use ….”
As suggested by the referee, to establish the sensitivity and specificity of a diagnostic test, it is indeed practical to use the Area Under the Receiver Operating Characteristic (ROC) curve (AUC). A ROC curve is a plot of the true positive rate (Sensitivity) in function of the false positive rate (100-Specificity) for different cut-off points of a parameter. Determining properly the sensitivity and specificity of a test thus requires large collections of samples which are known to be either certainly positive or certainly negative, which we did not have access to.

3. Are there any cross-reactivity with the other spike proteins from other CoVs? If so, what is the level of cross-reactivity?

Response: To assess cross-reactivity with other CoVs, we would have needed either Jurkat cells expressing the spike proteins from other CoVs, or sera with known reactivity against CoVs. Since we did not have access to such cells or sera, we were not in a position to address such a question.

4. While the authors have showed that the flow-based assay has a more dynamic range, there is

insufficient data showing that it is "more sensitive", as stated in the abstract. The authors should reflect this in the text.

Response: In the abstract, we do not state that the Jurkat-S&R-flow test is more sensitive than the ELISA, but “at least as sensitive”. On the other hand, we state that it is more sensitive than the HAT test, which it clearly is since there are more than a dozen samples on figure 2 that were positive with either or both ELISA and Jurkat-S&R-flow but were negative by HAT.
Of note, we have recently described an improved protocol, called HAT-field, which significantly improves the sensitivity of HAT, albeit at the cost of decreased specificity (https://doi.org/10.1101/2022.01.14.22268980)

5. Is trimer or monomer Spike expressed on the surface of the cells?

Response: Several studies have shown that, when the spike protein is expressed in human cells after transfection or transduction, it is in its native trimeric form at the cells’ surface and can even cause fusion with cells expressing the ACE2 receptor. This has now been clarified in the introduction section.

6. While there are significant advantages of the flow-based assay, the authors should discuss the limitations of a flow-based assay as a serological assay, especially for sero-surveillance and cohort studies. For instance, HTS application is usually limited for cell-based assays. In addition, while the assay is relatively cheap, it is worth nothing that the cytometer is an expensive equipment that not all laboratories have.

Response: We bring the referee’s attention to the fact that those points are discussed at the end of the introduction (line 161-165) : “ Since the Jurkat-flow test calls for the use of both a flow cytometer and cells obtained by tissue culture, it is clearly not destined to be used broadly in a diagnostic context, but its simplicity, modularity, and performances both in terms of sensitivity and quantification capacities should prove very useful for research labs working on characterizing antibody responses directed against SARS-2, both in humans and animal models. “

Minor concerns:

1. Figure 1 - text and numbers in the FACS plots are too small. Please adjust. In addition, for some of the FACS plots shown (eg. neg cont and serum 20/130), the population is right at the axis. Please pan the x-axis to allow better visualisation.
2. Figure 3A - please label axis.
3. Figure S2 - please label axis.
4. In general, please check through all figures for axis labels and also adjust the front size. For most, the text is too small.

Response: Sizes of numbers and text increased, and axis labels added in all figures

***Reviewer #1 (Significance (Required))**:*

As already discussed by the authors, there have already been quite a number of studies that have demonstrated the advantages of a flow-based assay for serological analysis for SARS-CoV-2. However, Ribes et al showed a new way to separate out alloreactivity from specific staining, which is important in reducing false positivity in serological assay. As more and more people receive their vaccination, there is a significant interest in immune-monitoring following vaccination. Given the more dynamic range of the flow-based assay, this is one good way to monitor antibody response.

Expertise*: My research interest focuses on the study of SARS-CoV-2 antibody responses following infection or vaccination.*

Reviewer #2 *(Evidence, reproducibility and clarity (Required)):*

In this paper, Joly and colleagues make use of a flow cytometry-based assay to measure in a reliable and sensitive manner the presence of IgG, IgA and IgM in blood samples from post-COVID human patients and also from laboratory (mouse and hamster) and domestic animals (dogs and cats). They find that the test is appropriate to detect the presence of humoral immunity in all species tested.
The manuscript is clearly written and the Figures are clearly presented. The experiments with rodente deliberately infected with inactivated SARS-CoV-2 shows (Fig. 3) that the method is reliable and able to clearly discriminate positive from negative sera. Interestingly, dogs and cats were sampled from households in which the owners had been found to have passed COVID-19 by PCR. Among this cohort of house animals they find more than 90% seroconversion for dogs and slightly less than 30% of clear seroconversion in cats.
We find however that the manuscript would benefit by establishing a clear cut-off value of "Specific Stain" for dogs and cats (Fig. 3). This could be implemented by including data from pre-COVID dog and cat sera or in its defect, sera from those species collected at households in which their owners were vaccinated and did not pass the infection. Another point of criticism that could be resolved is that the channels for flow cytometry in Figure 1 do not seem to be adequately compensated and there is evidence of some cross-contamination between FL1 and FL3.

Responses: We thank the referee for bringing our attention to the fact that we had presented the data on sera from cats and dogs in a confusing manner, which led the referee to believe that the sets of samples presented were representative of the population of animals whose owner had tested positive for Covid-19. In fact, for this experiment, which was only ever intended as a preliminary proof of concept that the test could be adapted very simply to companion animals, we used sets of sera which we knew would contain approximately 50 % of positive and 50 % negative samples because they had previously been screened by sero-neutralisation (incidentally, a manuscript by Bessière *et al.*, describing that work on sera from 131 cats and 156 dogs, has very recently been submitted for publication). To prevent possible confusions, we have now reworded the description of this proof of concept experiment, in the legend of figure 3, the text, and the methods section.

Regarding the question of a clear cut-off value, as when using human samples, we would suggest using a value of 40 for the instruments settings we used, corresponding to an RSS of 20 (i.e. 20 fold the value of the negative control). With such a value, it can be seen that one cat serum would be considered positive whilst showing no neutralising activity, but one dog serum which showed weak neutralising activity would be considered negative. If anything, this example highlights the difficulty in setting a precise cut off value for any biological test.

Regarding the question of inadequate compensation between channels 1 and 3, this is due to the fact that the Cellquest software does not allow for FL1/FL3 compensation, which is explained in the figure legend (see lines 208-210). We decided to simply draw the gates as they appear on figure 1 because attempts at post-acquisition compensation using the Flowjo software did not give satisfactory results. Incidentally, no compensation is required when samples are acquired on a Fortessa flow cytometer, where mCherry can be excited by a different laser (see figure S1) or if one uses the Jurkat-S&G-flow version of the test as in figure 3D for hamster sera (using Jurkat-GFP as negative control, and secondary antibodies conjugated to Alexa 488).

<u>Minor points</u>:

-Figure 1.- Please describe the y- and x-axis. Such as they are is difficult to find out.

Response: Done

-It would be advisable to mention in Materials and Methods (page 22) how blood was collected from cats and dogs.

Response: We thank the referee for highlighting this, and have now provided the information in the relevant method section.

-Line 856, page 22, "ad libidum" should be "ad libitum"

Response: We thank the referee for spotting this typo, which has been corrected

Reviewer #2 (Significance (Required))*:*

This is another step in the implementation of flow cytometry tests, instead of ELISA or CLIA serological tests based on the use of recombinant proteins, as a more sensitive and reliable method. The description of the high frequency of human-domestic animal transfer of SARS-CoV-2 will also add to the idea that it is humans who transmit the virus to those animals.